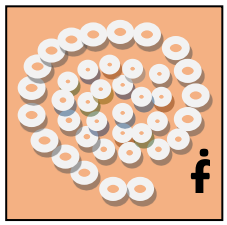

International Journal of Mathematical Analysis and Modelling

(Formerly Journal of the Nigerian Society for Mathematical Biology)

Volume 8 Issue 2, 2025

ISSN (Print): 2682 - 5694
ISSN (Online): 2682 – 5708
www.tnsmb.org

Age-structured deterministic model for the dynamics of Hepatitis B Virus in Nigeria incorporating vertical and horizontal transmission

F.C. Eze*and M.U. Uwaezuoke†

Abstract

This study introduces an age-structured deterministic model for the transmission dynamics of the Hepatitis B Virus (HBV) in Nigeria, accounting for both vertical (mother-to-child) and horizontal (person-to-person) transmission pathways. The population is categorized into children and adults to reflect differences in transmission and intervention effects. Analytical outcomes demonstrate the non-negativity of solutions and the existence of an invariant region, confirming the model's biological validity. The disease-free equilibrium (DFE) and the basic reproduction number (R_0) were determined using the next generation matrix approach. The local and global stability of the DFE were assessed using the Jacobian and Castillo–Chavez and Song methods, respectively, while the global stability of the endemic equilibrium was verified through a Lyapunov function. An optimal control problem was developed to examine three intervention strategies: childhood vaccination (u_1), adult catch-up vaccination (u_2), and birth-dose vaccination (u_3). Numerical simulations indicated that increasing childhood vaccination coverage results in an immediate reduction of acute infections among children and a delayed yet significant decline among adults through herd effects. Adult catch-up vaccination leads to a rapid decrease in acute infections and a gradual reduction in chronic cases, although some persistence occurs due to slow clearance and progression rates. Improved birth-dose vaccination demonstrated the most significant impact, preventing vertical transmission and moving the system toward near-elimination levels. Long-term simulations suggested that HBV reaches an endemic equilibrium under current conditions but could move towards elimination with sustained vaccination efforts. The analysis indicates that age-specific interventions, particularly universal birth-dose and intensified childhood vaccination, represent effective and sustainable strategies for controlling and eventually eliminating HBV in high-endemic regions such as Nigeria.

Keywords and phrases: age-structured model; hepatitis b virus; basic reproduction number; optimal control; vaccination strategies

1 Introduction

Hepatitis B virus (HBV) infection poses a significant public health challenge, especially in sub-Saharan Africa, where the disease is highly endemic and a major contributor to morbidity and mortality related to liver cirrhosis and hepatocellular carcinoma (HCC). According to the World Health Organization (WHO), approximately 1.1 million deaths from hepatitis B-related causes occurred globally in 2022, with the African Region experiencing a disproportionately high impact [1]. Nigeria, as the most populous country in Africa, is particularly affected by this epidemic. The estimated national HBsAg seroprevalence ranges from 8.1% to 13.6% among the general population, classifying the country as highly endemic, which means that over 18 million Nigerians are living with chronic HBV infection [2, 3]. This elevated prevalence results in a significant, often underappreciated health and economic

*Corresponding Author; E-mail:ezefrankline@imsuonline.edu.ng; Department of Mathematics, Imo State University Owerri, Nigeria

†Department of Mathematics, Imo State University, Owerri Nigeria; E-mail: uwaezuokemartin@gmail.com

burden, placing additional strain on a healthcare system already facing challenges from other infectious diseases such as malaria, HIV, and tuberculosis.

The transmission dynamics of HBV in Nigeria, similar to many high-endemic areas, are influenced by two main pathways: vertical (mother-to-child) and horizontal transmission. Vertical transmission happens when an infected mother, especially one with a high viral load (often indicated by being HBeAg-positive), transmits the virus to her newborn during childbirth. This method is highly effective, with a risk exceeding 90% without any preventive measures[1].The consequences are significant; more than 90% of infants infected perinatally will develop a chronic infection, creating a lifelong reservoir of the virus and a considerable risk of future liver complications [4].Horizontal transmission refers to the spread of the virus through contact with infected blood or body fluids. In Nigeria, this is particularly prevalent in early childhood (under 5 years) and occurs through methods such as close contact with infected family members, the use of unsterilized sharp objects in traditional practices, and iatrogenic transmission in healthcare environments that have inadequate infection control measures [5]. The age at which an infection occurs is the most significant factor in determining whether it will become chronic. Infections in adults are generally acute and resolve on their own, with a chronicity risk of less than 5%. However, for children under the age of five, the risk of chronicity increases to 20-30%, and for perinatal infections, this risk exceeds 90% [6].

The inclusion of the hepatitis B vaccine in the WHO's Expanded Programme on Immunization (EPI) has been a key component of global prevention initiatives. The most effective approach involves administering a monovalent birth dose (HepB-BD) within 24 hours after birth, along with at least two additional doses. This vaccination schedule is more than 95% effective in preventing perinatal and early childhood transmission [7].Nigeria incorporated the pentavalent vaccine, which safeguards against diphtheria, tetanus, pertussis, Haemophilus influenzae type b, and hepatitis B, into its national routine immunization schedule in 2012. Nonetheless, the coverage and timeliness of these vaccines, especially the important birth dose, are still lacking and display considerable regional variations [8]. As of 2022, the coverage of the HepB-BD in Nigeria was estimated to be 55%, which is significantly below the global average and the WHO 2030 target of 90% [9]. Barriers include low rates of deliveries in healthcare facilities, logistical challenges in vaccine storage and distribution, a lack of awareness among mothers and healthcare workers, and socio-cultural factors [10].

Hepatitis B is a DNA virus that is recognized as a considerable global health concern *Hepadnaviridae*. As of 2019, it is estimated that around 296 million individuals were living with chronic hepatitis B infection, leading to approximately 820,000 deaths each year from complications like cirrhosis and hepatocellular carcinoma (HCC) [1]. The distribution of the disease varies significantly across regions. The greatest impact is seen in the WHO African Region and the Western Pacific Region, where prevalence rates can exceed 8% [11]. In these areas with high rates of infection, the main modes of transmission are perinatal and horizontal transmission during early childhood.

Nigeria is notable within Africa for its substantial population and significant endemicity. A systematic review and meta-analysis by [2] reported a pooled HBsAg prevalence of 13.6% among Nigerians, with elevated rates noted in the northern regions. Recent studies at the state level continue to indicate this considerable burden. A study conducted by [3] in Anambra State, South-Eastern Nigeria, found an HBsAg prevalence of 8.1% among pregnant women, who are an important group concerning vertical transmission. The natural history of HBV in Nigeria typically shows a high rate of chronic infection due to childhood exposure, which contributes to a significant number of individuals living with chronic infection and at risk for progressive liver disease over their lifetime. Consequently, hepatocellular carcinoma (HCC) is a major cause of cancer mortality in the country, with HBV infection being the primary causative factor [12]. The economic impact is significant, including direct medical expenses for the treatment of chronic liver disease and HCC, as well as indirect costs related to lost productivity and early mortality, although this is not well quantified in Nigeria.

Vertical transmission (mother-to-child transmission) is a significant transmission route and a key factor in the epidemic in Nigeria. The risk of mother-to-child transmission is directly related to the mother's viral load. Mothers who are HBeAg-positive, often characterized by high levels of viral

replication, can transmit the virus to their newborns with an efficiency of 70-90% [13]. Without post-exposure prophylaxis, more than 90% of these infected infants are likely to become chronic carriers. The prevention of mother-to-child transmission (MTCT) relies on a three-part strategy: universal screening of pregnant women for HBsAg, administering the HepB-BD to all newborns within 24 hours of birth, and providing Hepatitis B Immune Globulin (HBIG) to infants born to HBsAg-positive mothers. The most recent WHO guidelines also suggest tenofovir antiviral prophylaxis for highly viremic pregnant women to further decrease the risk of transmission [14]. In Nigeria, the implementation of this comprehensive strategy is hindered by low attendance at antenatal care, restricted access to HBsAg testing, and significantly low coverage of HepB-BD [10]. Horizontal transmission during childhood is a significant source of infection for children under five in areas with high endemicity, such as Nigeria. This type of transmission happens through close contact with household members who are infected, likely through exposure to infected blood or bodily fluids via minor cuts or scratches, or through sharing contaminated items like toothbrushes or razors [5]. Other important routes include the use of unsterilized instruments in traditional practices such as scarification and circumcision, as well as iatrogenic transmission in environments with insufficient infection control. The intensity of infection for this pathway is highly dependent on age, with the highest rates occurring in early childhood. Transmission in adults primarily occurs through sexual contact, unsafe medical injections, blood transfusions (despite improvements in screening), and among people who inject drugs (PWID) in Nigeria. [15]. Adult-acquired infections are generally less prone to becoming chronic, but they still add to the total number of infections and can lead to considerable acute illness. This complex system of transmission, which is significantly influenced by age, highlights the importance of including a child-adult age structure in any realistic model for Nigeria.

Mathematical models have been widely utilized to analyze HBV dynamics and control. Initial foundational models by [23] laid the groundwork for infectious disease modeling. The field progressed with the incorporation of age structure, which is a significant development for HBV. The work in [24] were among the pioneers in creating an age-structured model, illustrating its importance for accurately forecasting the effects of vaccination, given that the force of infection and the risk of chronicity are highly influenced by age.

The explicit inclusion of vertical transmission represents a notable advancement. Models that treat all new infections as the same do not adequately reflect an important factor in the epidemic. The work in [27] created a model that distinguishes between vertical and horizontal transmission, indicating that while vaccinating infants of carrier mothers is effective, comprehensive coverage of routine infant immunization is ultimately necessary for eradication. More recently, [25] utilized a stochastic model to demonstrate that in areas with high prevalence, ongoing vertical transmission can maintain the epidemic for decades, even with substantial infant vaccine coverage, emphasizing the necessity for enhanced prevention of mother-to-child transmission (PMTCT).

While these global models offer important insights, their parameters, such as transmission rates and age-specific forces of infection, typically do not directly apply to Nigeria. Limited research has specifically examined HBV modeling in this region. A review by (ABC) regarding mathematical models for viral hepatitis in Africa identified a significant lack of models for HBV, despite its considerable burden. This indicates a notable gap in knowledge. The few existing models for Nigeria generally do not provide the detailed information necessary for effective policy planning, such as a clear distinction between vertical and horizontal transmission or a nuanced age structure that separates children from adults.

The current literature indicates various significant gaps that this research seeks to address:

1. **Nigeria-Specific Modeling:** There is a noticeable shortage of dynamic transmission models for HBV that are tailored with Nigerian demographic, epidemiological, and programmatic data. Using models designed for other regions may result in inaccurate predictions for Nigeria.

2. **Granular Age Structure and Transmission Pathways:** Numerous models utilize broad age categories. A model that specifically divides the population into “Children” and “Adults” and care-

fully includes distinct factors for vertical and horizontal transmission is necessary to accurately represent the fundamental dynamics of HBV in Nigeria.

3. **Focus on the Birth Dose Gap:** Previous models for Nigeria have not specifically quantified the long-term epidemiological impact of the country's low HepB-BD coverage or projected the benefits of addressing this gap.

4. **Policy Evaluation for WHO 2030 Goals:** There is a need for models that can project Nigeria's progress towards the WHO 2030 elimination targets under both current and improved intervention scenarios, offering a quantitative foundation for resource allocation and strategy improvement.

This study aims to address existing gaps. By creating a compartmental model that combines a complex structure (including age and dual transmission pathways) and is based on local Nigerian data, it will serve as a useful, context-specific resource for public health decision-making. The findings will provide essential evidence to support enhanced PMTCT services, improved routine immunization, and focused adult catch-up vaccination efforts, contributing to the objective of eradicating HBV as a public health concern in Nigeria.

2 Model Formulation

To address the critical gaps identified in the literature, we develop a deterministic compartmental model that stratifies the Nigerian population into two primary age groups: **Children (0-14 years)** and **Adults (15+ years)**. This structure captures the essential differences in transmission dynamics, disease progression, and intervention access between these groups. The model explicitly incorporates both horizontal and vertical transmission pathways and details the vaccination cascade, with particular emphasis on the birth dose.

2.1 Model Assumptions

1. The population is divided into two mutually exclusive age groups: Children (C) and Adults (A).
2. Only adults give birth, and births occur into the susceptible children compartment.
3. Vertical transmission can occur from both acutely and chronically infected mothers.
4. The hepatitis B vaccine birth dose (HepB-BD) is administered within 24 hours of birth with coverage ϕ, and provides protection against both vertical and early horizontal transmission.
5. Routine childhood vaccination occurs at a rate θ_c for susceptible children.
6. Vaccine-induced immunity may wane over time.
7. Individuals age from the children to adult compartments at a constant rate ρ.
8. Horizontal transmission follows standard incidence, with different contact rates for children and adults.

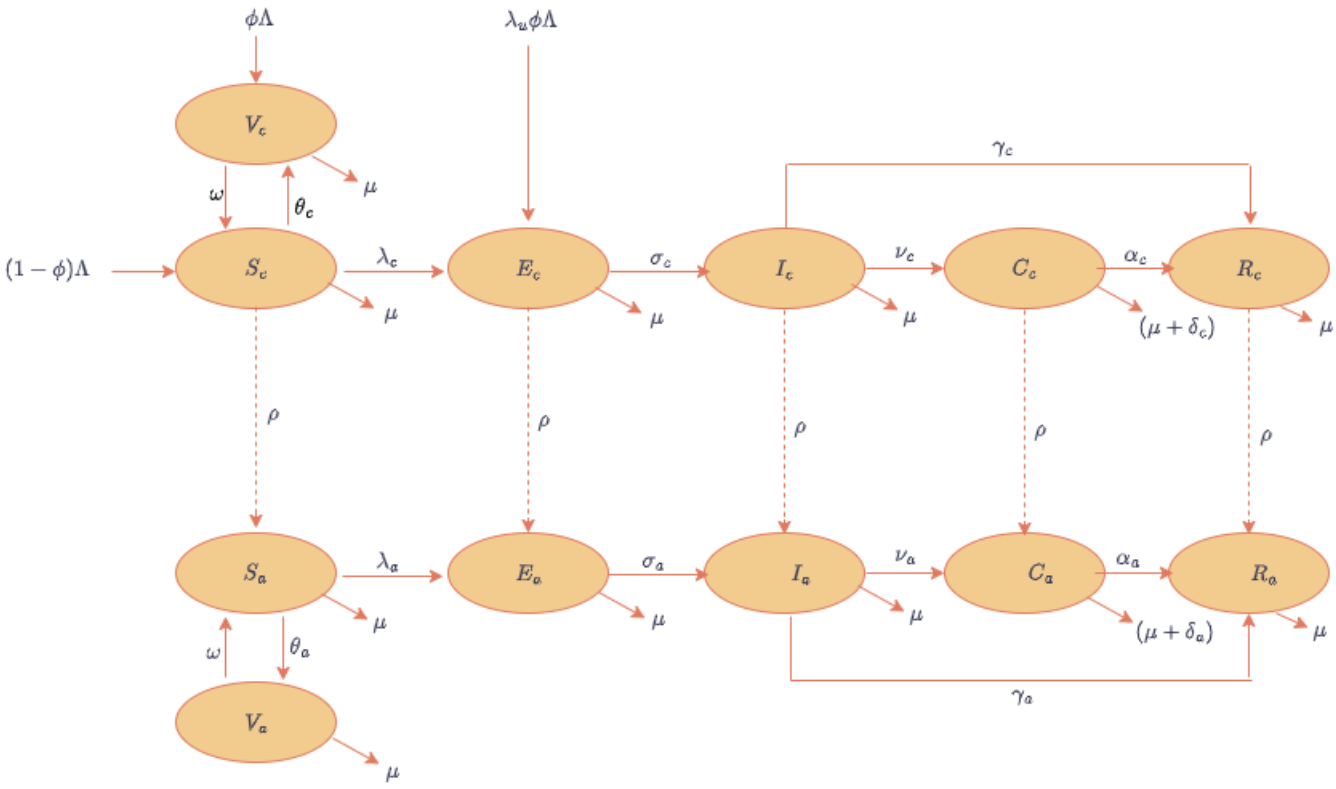

Figure 1: Model Flow Chart

The total population is given by:

$$\begin{aligned} N_c(t) &= S_c(t) + V_c(t) + E_c(t) + I_c(t) + C_c(t) + R_c(t) \\ N_a(t) &= S_a(t) + V_a(t) + E_a(t) + I_a(t) + C_a(t) + R_a(t) \\ N(t) &= N_c(t) + N_a(t) \\ \Lambda(t) &= \mu N_a(t) \end{aligned}$$

2.2 Model Equations

$$\frac{dS_c}{dt} = (1-\phi)\Lambda - (\lambda_c + \theta_c + \rho + \mu)S_c + \omega V_c \tag{1}$$

$$\frac{dS_a}{dt} = \rho S_c - (\lambda_a + \theta_a + \mu)S_a + \omega V_a \tag{2}$$

$$\frac{dV_c}{dt} = \phi\Lambda + \theta_c S_c - (\omega + \rho + \mu)V_c \tag{3}$$

$$\frac{dV_a}{dt} = \rho V_c + \theta_a S_a - (\omega + \mu)V_a \tag{4}$$

$$\frac{dE_c}{dt} = \lambda_c S_c + \lambda_v \phi\Lambda - (\sigma_c + \rho + \mu)E_c \tag{5}$$

$$\frac{dE_a}{dt} = \lambda_a S_a + \rho E_c - (\sigma_a + \mu)E_a \tag{6}$$

$$\frac{dI_c}{dt} = \sigma_c E_c - (\gamma_c + \nu_c + \rho + \mu)I_c \tag{7}$$

$$\frac{dI_a}{dt} = \sigma_a E_a + \rho I_c - (\gamma_a + \nu_a + \mu)I_a \tag{8}$$

$$\frac{dC_c}{dt} = \nu_c I_c - (\alpha_c + \rho + \mu + \delta_c)C_c \tag{9}$$

$$\frac{dC_a}{dt} = \nu_a I_a + \rho C_c - (\alpha_a + \mu + \delta_a)C_a \tag{10}$$

$$\frac{dR_c}{dt} = \gamma_c I_c + \alpha_c C_c - (\rho + \mu)R_c \tag{11}$$

$$\frac{dR_a}{dt} = \gamma_a I_a + \alpha_a C_a + \rho R_c - \mu R_a \tag{12}$$

where the force of infection for horizontal transmission is modeled using standard incidence:

$$\lambda_c = \beta_c \left(\frac{I_c + \eta_c C_c + I_a + \eta_a C_a}{N} \right)$$

$$\lambda_a = \beta_a \left(\frac{I_c + \eta_c C_c + I_a + \eta_a C_a}{N} \right)$$

And the term for vaccine failure in vertical transmission is:

$$\lambda_v = p_v \left(\frac{I_a + \eta_v C_a}{N_a} \right)$$

where $\lambda_c(t)$ is the force of infection for horizontal transmission in children per year, $\lambda_a(t)$ is the force of infection for horizontal transmission in adults per year, and $\lambda_v(t)$ is the force of vertical transmission from infected mothers to newborns per year.

Relative Vertical Transmission Risk Factor

- This multiplier accounts for the difference in vertical transmission risk between chronically infected mothers (C_a) and acutely infected mothers (I_a)

- If $\eta_v = 1$, chronic and acute mothers have equal transmission risk
- If $\eta_v > 1$, chronic mothers have higher transmission risk (biologically plausible due to longer duration of infection)
- If $\eta_v < 1$, chronic mothers have lower transmission risk
- Typical range: 0.8 to 1.2 based on viral load characteristics

Table 1: State Variables for the Unified HBV Model

Variable	Meaning	Unit
$S_c(t)$	Number of susceptible children (0-14 years)	individuals
$V_c(t)$	Number of vaccinated children with immunity	individuals
$E_c(t)$	Number of exposed/latently infected children	individuals
$I_c(t)$	Number of acutely infectious children	individuals
$C_c(t)$	Number of chronically infected children	individuals
$R_c(t)$	Number of recovered children with natural immunity	individuals
$S_a(t)$	Number of susceptible adults (15+ years)	individuals
$V_a(t)$	Number of vaccinated adults with immunity	individuals
$E_a(t)$	Number of exposed/latently infected adults	individuals
$I_a(t)$	Number of acutely infectious adults	individuals
$C_a(t)$	Number of chronically infected adults	individuals
$R_a(t)$	Number of recovered adults with natural immunity	individuals

Table 2: Description of Model Parameters

Parameter	Description	Unit
Λ	Natural birth rate	per year
μ	Natural death rate	per year
ρ	Aging rate from children to adults (1/15)	per year
β_c, β_a	Effective contact rates for children and adults	per year
η_c, η_a	Relative infectiousness of chronic carriers	dimensionless
ϕ	Hepatitis B birth dose (HepB-BD) coverage	dimensionless
θ_c, θ_a	Routine and catch-up vaccination rates	per year
ω	Waning rate of vaccine immunity	per year
σ_c, σ_a	Progression rate from exposed to acute infection	per year
γ_c, γ_a	Recovery rate from acute infection	per year
ν_c, ν_a	Progression rate to chronic infection	per year
α_c, α_a	Recovery rate from chronic infection	per year
δ_c, δ_a	Disease-induced mortality for chronic infections	per year
p_v	Probability of vertical transmission from infected mothers	dimensionless
η_v	Relative risk of vertical transmission from chronic vs. acute mothers	dimensionless

3 Mathematical Analysis of the Age-Structured HBV Model

3.1 Invariant Region

Theorem 3.1. *The feasible region for the HBV model given by:*

$$\Omega = \left\{ (S_c, V_c, E_c, I_c, C_c, R_c, S_a, V_a, E_a, I_a, C_a, R_a) \in \mathbb{R}_+^{12} : N_c + N_a \leq \frac{\mu \bar{N}_a}{\mu} \right\}$$

is positively invariant and attracting for all $t \geq 0$.

Proof. The total population dynamics are given by:

$$\begin{aligned} \frac{dN}{dt} &= \frac{dN_c}{dt} + \frac{dN_a}{dt} \\ &= \Lambda - \mu N - \delta_c C_c - \delta_a C_a \\ &\leq \mu \bar{N}_a - \mu N \end{aligned}$$

Solving this differential inequality:

$$\begin{aligned} \frac{dN}{dt} + \mu N &\leq \mu \bar{N}_a \\ N(t) &\leq N(0)e^{-\mu t} + \bar{N}_a(1 - e^{-\mu t}) \\ \limsup_{t \to \infty} N(t) &\leq \bar{N}_a \end{aligned}$$

where $\bar{N}_a$ is the equilibrium adult population. Since all state variables represent population sizes, they must be non-negative. Therefore, Ω is positively invariant.

3.2 Non-negativity of Solutions

Theorem 3.2. *Given the initial states*

$$S_c(0) \geq 0,\ S_a(0) \geq 0,\ V_c(0) \geq 0,\ V_a(0) \geq 0,\ E_c(0) \geq 0,\ E_a(0) \geq 0,\ I_c(0) \geq 0,\ I_a(0) \geq 0,\ C_c(0) \geq 0,\ C_a(0) \geq 0$$

then the solutions

$$\big(S_c(t),\, S_a(t),\, V_c(t),\, V_a(t),\, E_c(t),\, E_a(t),\, I_c(t),\, I_a(t),\, C_c(t),\, C_a(t),\, R_c(t),\, R_a(t)\big)$$

of model (1) remain non-negative for all time $t > 0$.

Proof. Consider the feasible region

$$\Omega = \Big\{ (S_c, S_a, V_c, V_a, E_c, E_a, I_c, I_a, C_c, C_a, R_c, R_a) \in \mathbb{R}_+^{12} \;\Big|\; S_c, S_a, V_c, V_a, E_c, E_a, I_c, I_a, C_c, C_a, R_c, R_a \geq 0 \Big\}.$$

The model equations governing these state variables are continuous and differentiable in Ω. To show non-negativity, we examine each equation on the boundary of Ω: For each differential equation of the form:

$$\frac{dX}{dt} + B(t)X = A(t)$$

the solution is given by:

$$X(t) = X(0)e^{-\int_0^t B(s)\,ds} + \int_0^t A(\tau)e^{-\int_\tau^t B(s)\,ds}\,d\tau$$

If $X(0) \geq 0$, $A(t) \geq 0$ for all $t \geq 0$, and $B(t)$ is bounded, then $X(t) \geq 0$ for all $t \geq 0$.

From the first equation of model

$$\frac{dS_c}{dt} = (1-\phi)\Lambda - (\lambda_c + \theta_c + \rho + \mu)S_c + \omega V_c \tag{13}$$

$$\frac{dS_c}{dt} + (\lambda_c + \theta_c + \rho + \mu)S_c = (1-\phi)\Lambda + \omega V_c$$

Solution:

$$S_c(t) = S_c(0)e^{-\int_0^t (\lambda_c(s)+\theta_c+\rho+\mu)\,ds} + \int_0^t [(1-\phi)\Lambda(\tau) + \omega V_c(\tau)]e^{-\int_\tau^t (\lambda_c(s)+\theta_c+\rho+\mu)\,ds}\,d\tau$$

Since $S_c(0) \geq 0$, $(1-\phi)\Lambda(\tau) \geq 0$, $\omega V_c(\tau) \geq 0$, and the exponential terms are positive
Hence $S_c(t) \geq 0$.

From the second equation of model (1)

$$\frac{dS_a}{dt} = \rho S_c - (\lambda_a + \theta_a + \mu)S_a + \omega V_a \tag{14}$$

$$\frac{dS_a}{dt} + (\lambda_a + \theta_a + \mu)S_a = \rho S_c + \omega V_a$$

Solution:

$$S_a(t) = S_a(0)e^{-\int_0^t (\lambda_a(s)+\theta_a+\mu)\,ds} + \int_0^t [\rho S_c(\tau) + \omega V_a(\tau)]e^{-\int_\tau^t (\lambda_a(s)+\theta_a+\mu)\,ds}\,d\tau$$

Since $S_a(0) \geq 0$, $\rho S_c(\tau) \geq 0$, $\omega V_a(\tau) \geq 0$, $S_a(t) \geq 0$.

From the third equation of model (1)

$$\frac{dV_c}{dt} = \phi\Lambda + \theta_c S_c - (\omega + \rho + \mu)V_c \tag{15}$$

$$\frac{dV_c}{dt} + (\omega + \rho + \mu)V_c = \phi\Lambda + \theta_c S_c$$

Solution:

$$V_c(t) = V_c(0)e^{-\int_0^t (\omega+\rho+\mu)\,ds} + \int_0^t [\phi\Lambda(\tau) + \theta_c S_c(\tau)]e^{-\int_\tau^t (\omega+\rho+\mu)\,ds}\,d\tau$$

Since $V_c(0) \geq 0$, $\phi\Lambda(\tau) \geq 0$, $\theta_c S_c(\tau) \geq 0$, $V_c(t) \geq 0$.

From the fourth equation of model (1)

$$\frac{dV_a}{dt} = \rho V_c + \theta_a S_a - (\omega + \mu)V_a \tag{16}$$

$$\frac{dV_a}{dt} + (\omega + \mu)V_a = \rho V_c + \theta_a S_a$$

Solution:

$$V_a(t) = V_a(0)e^{-\int_0^t (\omega+\mu)\,ds} + \int_0^t [\rho V_c(\tau) + \theta_a S_a(\tau)]e^{-\int_\tau^t (\omega+\mu)\,ds}\,d\tau$$

Since $V_a(0) \geq 0$, $\rho V_c(\tau) \geq 0$, $\theta_a S_a(\tau) \geq 0$, $V_a(t) \geq 0$.

From the fifth equation of model (1)

$$\frac{dE_c}{dt} = \lambda_c S_c + \lambda_v \phi\Lambda - (\sigma_c + \rho + \mu)E_c \tag{17}$$

$$\frac{dE_c}{dt} + (\sigma_c + \rho + \mu)E_c = \lambda_c S_c + \lambda_v \phi\Lambda$$

Solution:

$$E_c(t) = E_c(0)e^{-\int_0^t (\sigma_c+\rho+\mu)\,ds} + \int_0^t [\lambda_c(\tau)S_c(\tau) + \lambda_v(\tau)\phi\Lambda(\tau)]e^{-\int_\tau^t (\sigma_c+\rho+\mu)\,ds}\,d\tau$$

Since $E_c(0) \geq 0$, $\lambda_c(\tau) \geq 0$, $S_c(\tau) \geq 0$, $\lambda_v(\tau) \geq 0$, $\phi\Lambda(\tau) \geq 0$, $E_c(t) \geq 0$.

From the sixth equation of model (1)

$$\frac{dE_a}{dt} = \lambda_a S_a + \rho E_c - (\sigma_a + \mu)E_a \tag{18}$$

$$\frac{dE_a}{dt} + (\sigma_a + \mu)E_a = \lambda_a S_a + \rho E_c$$

Solution:

$$E_a(t) = E_a(0)e^{-\int_0^t (\sigma_a+\mu)\,ds} + \int_0^t [\lambda_a(\tau)S_a(\tau) + \rho E_c(\tau)]e^{-\int_\tau^t (\sigma_a+\mu)\,ds}\,d\tau$$

Since $E_a(0) \geq 0$, $\lambda_a(\tau) \geq 0$, $S_a(\tau) \geq 0$, $\rho E_c(\tau) \geq 0$, $E_a(t) \geq 0$.

From the seventh equation of model (1)

$$\frac{dI_c}{dt} = \sigma_c E_c - (\gamma_c + \nu_c + \rho + \mu)I_c \tag{19}$$

$$\frac{dI_c}{dt} + (\gamma_c + \nu_c + \rho + \mu)I_c = \sigma_c E_c$$

Solution:

$$I_c(t) = I_c(0)e^{-\int_0^t (\gamma_c+\nu_c+\rho+\mu)\,ds} + \int_0^t \sigma_c E_c(\tau)e^{-\int_\tau^t (\gamma_c+\nu_c+\rho+\mu)\,ds}\,d\tau$$

Since $I_c(0) \geq 0$, $\sigma_c E_c(\tau) \geq 0$, $I_c(t) \geq 0$.

From the eighth equation of model (1)

$$\frac{dI_a}{dt} = \sigma_a E_a + \rho I_c - (\gamma_a + \nu_a + \mu)I_a \tag{20}$$

$$\frac{dI_a}{dt} + (\gamma_a + \nu_a + \mu)I_a = \sigma_a E_a + \rho I_c$$

Solution:

$$I_a(t) = I_a(0)e^{-\int_0^t (\gamma_a+\nu_a+\mu)\,ds} + \int_0^t [\sigma_a E_a(\tau) + \rho I_c(\tau)]e^{-\int_\tau^t (\gamma_a+\nu_a+\mu)\,ds}\,d\tau$$

Since $I_a(0) \geq 0$, $\sigma_a E_a(\tau) \geq 0$, $\rho I_c(\tau) \geq 0$, $I_a(t) \geq 0$.

From the ninth equation of model (1)

$$\frac{dC_c}{dt} = \nu_c I_c - (\alpha_c + \rho + \mu + \delta_c)C_c \tag{21}$$

$$\frac{dC_c}{dt} + (\alpha_c + \rho + \mu + \delta_c)C_c = \nu_c I_c$$

Solution:

$$C_c(t) = C_c(0)e^{-\int_0^t (\alpha_c+\rho+\mu+\delta_c)\,ds} + \int_0^t \nu_c I_c(\tau)e^{-\int_\tau^t (\alpha_c+\rho+\mu+\delta_c)\,ds}\,d\tau$$

Since $C_c(0) \geq 0$, $\nu_c I_c(\tau) \geq 0$, $C_c(t) \geq 0$.

From the tenth equation of model (1)

$$\frac{dC_a}{dt} = \nu_a I_a + \rho C_c - (\alpha_a + \mu + \delta_a)C_a \tag{22}$$

$$\frac{dC_a}{dt} + (\alpha_a + \mu + \delta_a)C_a = \nu_a I_a + \rho C_c$$

Solution:

$$C_a(t) = C_a(0)e^{-\int_0^t (\alpha_a+\mu+\delta_a)\,ds} + \int_0^t [\nu_a I_a(\tau) + \rho C_c(\tau)]e^{-\int_\tau^t (\alpha_a+\mu+\delta_a)\,ds}\,d\tau$$

Since $C_a(0) \geq 0$, $\nu_a I_a(\tau) \geq 0$, $\rho C_c(\tau) \geq 0$, $C_a(t) \geq 0$.

From the eleventh equation of model (1)

$$\frac{dR_c}{dt} = \gamma_c I_c + \alpha_c C_c - (\rho + \mu)R_c \tag{23}$$

$$\frac{dR_c}{dt} + (\rho + \mu)R_c = \gamma_c I_c + \alpha_c C_c$$

Solution:

$$R_c(t) = R_c(0)e^{-\int_0^t (\rho+\mu)\,ds} + \int_0^t [\gamma_c I_c(\tau) + \alpha_c C_c(\tau)]e^{-\int_\tau^t (\rho+\mu)\,ds}\,d\tau$$

Since $R_c(0) \geq 0$, $\gamma_c I_c(\tau) \geq 0$, $\alpha_c C_c(\tau) \geq 0$, $R_c(t) \geq 0$.

From the last equation of model (1)

$$\frac{dR_a}{dt} = \gamma_a I_a + \alpha_a C_a + \rho R_c - \mu R_a \tag{24}$$

$$\frac{dR_a}{dt} + \mu R_a = \gamma_a I_a + \alpha_a C_a + \rho R_c$$

Solution:

$$R_a(t) = R_a(0)e^{-\int_0^t \mu\,ds} + \int_0^t [\gamma_a I_a(\tau) + \alpha_a C_a(\tau) + \rho R_c(\tau)]e^{-\int_\tau^t \mu\,ds}\,d\tau$$

Since $R_a(0) \geq 0$, $\gamma_a I_a(\tau) \geq 0$, $\alpha_a C_a(\tau) \geq 0$, $\rho R_c(\tau) \geq 0$, $R_a(t) \geq 0$.

Thus, all state variables of the model remain non–negative for all $t > 0$ whenever the initial conditions are non–negative. Consequently, the model is biologically well–posed, and its feasible region ($\Omega \subset \mathbb{R}^{12}_+$) is positively invariant under the flow of the system.

3.3 Disease-Free Equilibrium (DFE)

The disease-free equilibrium (DFE) of the HBV model is given by setting all derivatives in the system (??) to zero and assuming the absence of infection in the population, that is,

$$E_c = E_a = I_c = I_a = C_c = C_a = 0.$$

At the DFE, the forces of infection vanish, hence

$$\lambda_c = \lambda_a = \lambda_v = 0.$$

At equilibrium,

$$S_c^* = \frac{(1-\phi)\Lambda(\omega+\rho+\mu)+\omega\phi\Lambda}{(\theta_c+\rho+\mu)(\omega+\rho+\mu)-\omega\theta_c}.$$

$$V_c^* = \frac{\phi\Lambda+\theta_c S_c^*}{\omega+\rho+\mu}.$$

$$S_a^* = \frac{\rho S_c^*(\omega+\mu)+\omega\rho V_c^*}{(\theta_a+\mu)(\omega+\mu)-\omega\theta_a},$$

and

$$V_a^* = \frac{\rho V_c^*+\theta_a S_a^*}{\omega+\mu}.$$

Therefore, the Disease-Free Equilibrium (DFE) is given by:

$$E_0 = (S_c^*, S_a^*, V_c^*, V_a^*, E_c^*, E_a^*, I_c^*, I_a^*, C_c^*, C_a^*, R_c^*, R_a^*),$$

where

$$E_c^* = E_a^* = I_c^* = I_a^* = C_c^* = C_a^* = R_c^* = R_a^* = 0,$$
$$S_c^*, V_c^*, S_a^*, V_a^* > 0$$

That is,

$$E_0 = (S_c^*, S_a^*, V_c^*, V_a^*, 0, 0, 0, 0, 0, 0, 0, 0),$$

The disease-free equilibrium (E_0) indicates a state in which there are no infections present in the child or adult populations, and the susceptible and vaccinated groups maintain a balance influenced by demographic and vaccination factors.

3.4 Basic Reproduction Number (R_0)

This represents the average number of secondary infections produced by one infected individual in a completely susceptible population, accounting for both horizontal and vertical transmission pathways across both age groups.

To compute the basic reproduction number R_0, we employ the next-generation matrix (NGM) approach [16]. We first identify the infected compartments as

$$X = (E_c, E_a, I_c, I_a, C_c, C_a)^T.$$

The system of equations for new infections and transitions among these compartments can be written as:

$$\frac{dX}{dt} = \mathcal{F}(X) - \mathcal{V}(X),$$

where $\mathcal{F}$ represents the rate of appearance of new infections and $\mathcal{V}$ represents the rate of transfer into and out of the infected compartments by all other means.

From the model equations, the new infection terms are given by:

$$\mathcal{F} = \begin{pmatrix} \lambda_c S_c^0 + \lambda_v \phi \Lambda^0 \\ \lambda_a S_a^0 \\ 0 \\ 0 \\ 0 \\ 0 \end{pmatrix},$$

where at the disease-free equilibrium (DFE),

$$E_c^0 = E_a^0 = I_c^0 = I_a^0 = C_c^0 = C_a^0 = 0,$$

and λ_c, λ_a, and λ_v are the forces of infection defined by:

$$\lambda_c = \beta_c \frac{I_c + \eta_c C_c + I_a + \eta_a C_a}{N},$$
$$\lambda_a = \beta_a \frac{I_c + \eta_c C_c + I_a + \eta_a C_a}{N},$$
$$\lambda_v = p_v \frac{I_a + \eta_v C_a}{N_a}.$$

The transition terms are given by:

$$\mathcal{V} = \begin{pmatrix} (\sigma_c + \rho + \mu) E_c \\ (\sigma_a + \mu) E_a - \rho E_c \\ (\gamma_c + \nu_c + \rho + \mu) I_c - \sigma_c E_c \\ (\gamma_a + \nu_a + \mu) I_a - \sigma_a E_a - \rho I_c \\ (\alpha_c + \rho + \mu + \delta_c) C_c - \nu_c I_c \\ (\alpha_a + \mu + \delta_a) C_a - \nu_a I_a - \rho C_c \end{pmatrix}.$$

Let F and V be the Jacobian matrices of $\mathcal{F}$ and $\mathcal{V}$ evaluated at the DFE.

$$F = \begin{pmatrix} 0 & 0 & \frac{\beta_c S_c^0}{N^0} & \frac{\beta_c S_c^0}{N^0} & \frac{\beta_c \eta_c S_c^0}{N^0} & \frac{\beta_c \eta_a S_c^0}{N^0} \\ 0 & 0 & \frac{\beta_a S_a^0}{N^0} & \frac{\beta_a S_a^0}{N^0} & \frac{\beta_a \eta_c S_a^0}{N^0} & \frac{\beta_a \eta_a S_a^0}{N^0} \\ 0 & 0 & 0 & 0 & 0 & 0 \\ 0 & 0 & 0 & 0 & 0 & 0 \\ 0 & 0 & 0 & 0 & 0 & 0 \\ 0 & 0 & 0 & 0 & 0 & 0 \end{pmatrix},$$

and

$$V = \begin{pmatrix} \sigma_c + \rho + \mu & 0 & 0 & 0 & 0 & 0 \\ -\rho & \sigma_a + \mu & 0 & 0 & 0 & 0 \\ -\sigma_c & 0 & \gamma_c + \nu_c + \rho + \mu & 0 & 0 & 0 \\ 0 & -\sigma_a & -\rho & \gamma_a + \nu_a + \mu & 0 & 0 \\ 0 & 0 & -\nu_c & 0 & \alpha_c + \rho + \mu + \delta_c & 0 \\ 0 & 0 & 0 & -\nu_a & -\rho & \alpha_a + \mu + \delta_a \end{pmatrix}.$$

$$V^{-1} = \begin{pmatrix} \frac{1}{k_1} & 0 & 0 & 0 & 0 & 0 \\ \frac{\rho}{k_1 k_2} & \frac{1}{k_2} & 0 & 0 & 0 & 0 \\ \frac{\sigma_c}{k_1 k_3} & 0 & \frac{1}{k_3} & 0 & 0 & 0 \\ \frac{\rho\sigma_c}{k_1 k_3 k_4} + \frac{\sigma_a \rho}{k_1 k_2 k_4} & \frac{\sigma_a}{k_2 k_4} & \frac{\rho}{k_3 k_4} & \frac{1}{k_4} & 0 & 0 \\ \frac{\nu_c \sigma_c}{k_1 k_3 k_5} & 0 & \frac{\nu_c}{k_3 k_5} & 0 & \frac{1}{k_5} & 0 \\ \frac{\rho\nu_c\sigma_c}{k_1 k_3 k_5 k_6} + \frac{\rho\nu_c\sigma_c}{k_1 k_3 k_4 k_6} + \frac{\nu_a\sigma_a\rho}{k_1 k_2 k_4 k_6} & \frac{\nu_a\sigma_a}{k_2 k_4 k_6} & \frac{\rho\nu_c}{k_3 k_4 k_6} + \frac{\rho\nu_c}{k_3 k_5 k_6} & \frac{\nu_a}{k_4 k_6} & \frac{\rho}{k_5 k_6} & \frac{1}{k_6} \end{pmatrix}$$

where

$$
\begin{aligned}
k_1 &= \sigma_c + \rho + \mu \\
k_2 &= \sigma_a + \mu \\
k_3 &= \gamma_c + \nu_c + \rho + \mu \\
k_4 &= \gamma_a + \nu_a + \mu \\
k_5 &= \alpha_c + \rho + \mu + \delta_c \\
k_6 &= \alpha_a + \mu + \delta_a
\end{aligned}
$$

$$
FV^{-1} = \begin{pmatrix}
F_{11} & F_{12} & F_{13} & F_{14} & F_{15} & F_{16} \\
F_{21} & F_{22} & F_{23} & F_{24} & F_{25} & F_{26} \\
0 & 0 & 0 & 0 & 0 & 0 \\
0 & 0 & 0 & 0 & 0 & 0 \\
0 & 0 & 0 & 0 & 0 & 0 \\
0 & 0 & 0 & 0 & 0 & 0
\end{pmatrix}
$$

where:

$$
\begin{aligned}
F_{11} &= \frac{\beta_c S_c^* \sigma_c}{N^* k_1 k_3} + \frac{\beta_a S_a^* \sigma_c \rho}{N^* k_1 k_3 k_4} + \frac{\beta_a S_a^* \sigma_a \rho}{N^* k_1 k_2 k_4} + \left(\frac{\beta_c S_c^*}{N^*} + \frac{\phi \Lambda p_v}{N_a^*}\right)\left(\frac{\rho \sigma_c}{k_1 k_3 k_4} + \frac{\sigma_a \rho}{k_1 k_2 k_4}\right) \\
F_{12} &= \frac{\beta_a S_a^* \sigma_a}{N^* k_2 k_4} + \left(\frac{\beta_c S_c^*}{N^*} + \frac{\phi \Lambda p_v}{N_a^*}\right)\frac{\sigma_a}{k_2 k_4} \\
F_{13} &= \frac{\beta_c S_c^*}{N^* k_3} + \frac{\beta_a S_a^* \rho}{N^* k_3 k_4} + \left(\frac{\beta_c S_c^*}{N^*} + \frac{\phi \Lambda p_v}{N_a^*}\right)\frac{\rho}{k_3 k_4} \\
F_{14} &= \frac{\beta_a S_a^*}{N^* k_4} + \left(\frac{\beta_c S_c^*}{N^*} + \frac{\phi \Lambda p_v}{N_a^*}\right)\frac{1}{k_4} \\
F_{15} &= \frac{\beta_c S_c^* \eta_c \nu_c}{N^* k_3 k_5} + \frac{\beta_a S_a^* \eta_c \rho \nu_c}{N^* k_3 k_4 k_6} + \frac{\beta_a S_a^* \eta_c \rho \nu_c}{N^* k_3 k_5 k_6} + \left(\frac{\beta_c S_c^* \eta_a}{N^*} + \frac{\phi \Lambda p_v \eta_v}{N_a^*}\right)\left(\frac{\rho \nu_c}{k_3 k_4 k_6} + \frac{\rho \nu_c}{k_3 k_5 k_6}\right) \\
F_{16} &= \frac{\beta_a S_a^* \eta_a \nu_a}{N^* k_4 k_6} + \left(\frac{\beta_c S_c^* \eta_a}{N^*} + \frac{\phi \Lambda p_v \eta_v}{N_a^*}\right)\frac{\nu_a}{k_4 k_6} \\
F_{21} &= \frac{\beta_a S_a^*}{N^* k_1 k_3} + \frac{\beta_a S_a^* \rho}{N^* k_1 k_3 k_4} + \frac{\beta_a S_a^* \sigma_a \rho}{N^* k_1 k_2 k_4} + \frac{\beta_a S_a^* \eta_c \nu_c \sigma_c}{N^* k_1 k_3 k_5} \\
&\quad + \frac{\beta_a S_a^* \eta_a}{N^*}\left(\frac{\rho \nu_c \sigma_c}{k_1 k_3 k_5 k_6} + \frac{\rho \nu_c \sigma_c}{k_1 k_3 k_4 k_6} + \frac{\nu_a \sigma_a \rho}{k_1 k_2 k_4 k_6}\right) \\
F_{22} &= \frac{\beta_a S_a^* \sigma_a}{N^* k_2 k_4} + \frac{\beta_a S_a^* \eta_a \nu_a \sigma_a}{N^* k_2 k_4 k_6} \\
F_{23} &= \frac{\beta_a S_a^*}{N^* k_3} + \frac{\beta_a S_a^* \rho}{N^* k_3 k_4} + \frac{\beta_a S_a^* \eta_c \nu_c}{N^* k_3 k_5} + \frac{\beta_a S_a^* \eta_a}{N^*}\left(\frac{\rho \nu_c}{k_3 k_4 k_6} + \frac{\rho \nu_c}{k_3 k_5 k_6}\right) \\
F_{24} &= \frac{\beta_a S_a^*}{N^* k_4} + \frac{\beta_a S_a^* \eta_a \nu_a}{N^* k_4 k_6} \\
F_{25} &= \frac{\beta_a S_a^* \eta_c}{N^* k_5} + \frac{\beta_a S_a^* \eta_a \rho}{N^* k_5 k_6} \\
F_{26} &= \frac{\beta_a S_a^* \eta_a}{N^* k_6}
\end{aligned}
$$

The basic reproduction number R_0 is the spectral radius (dominant eigenvalue) of FV^{-1}:

$$R_0 = \rho(FV^{-1})$$

Thus

$$R_0 = \frac{1}{2}\left(F_{11} + F_{22} + \sqrt{(F_{11} - F_{22})^2 + 4F_{12}F_{21}}\right)$$

3.5 Local Stability Analysis

Theorem 3.3 (Stability of DFE). *The disease-free equilibrium is locally asymptotically stable if $\mathcal{R}_0 < 1$ and unstable if $\mathcal{R}_0 > 1$.*

Proof: The Jacobian matrix of the system evaluated at the disease free equilibrium point.

We consider the Jacobian matrix

$$J(x) = \begin{pmatrix}
-(\lambda_c+\theta_c+\rho+\mu) & \frac{\partial(1-\phi)\Lambda}{\partial S_a} & \omega & \frac{\partial(1-\phi)\Lambda}{\partial V_a} & -S_c\frac{\partial\lambda_c}{\partial E_c} & -S_c\frac{\partial\lambda_c}{\partial E_a} & -S_c\frac{\partial\lambda_c}{\partial I_c} & -S_c\frac{\partial\lambda_c}{\partial I_a} & -S_c\frac{\partial\lambda_c}{\partial C_c} & -S_c\frac{\partial\lambda_c}{\partial C_a} & 0 & \frac{\partial(1-\phi)\Lambda}{\partial R_a} \\
\rho & -(\lambda_a+\theta_a+\mu) & 0 & \omega & 0 & -S_a\frac{\partial\lambda_a}{\partial E_a} & -S_a\frac{\partial\lambda_a}{\partial I_c} & -S_a\frac{\partial\lambda_a}{\partial I_a} & -S_a\frac{\partial\lambda_a}{\partial C_c} & -S_a\frac{\partial\lambda_a}{\partial C_a} & 0 & 0 \\
\theta_c & 0 & -(\omega+\rho+\mu) & \frac{\partial\phi\Lambda}{\partial V_a} & 0 & 0 & 0 & 0 & 0 & 0 & 0 & \frac{\partial\phi\Lambda}{\partial R_a} \\
0 & \theta_a & \rho & -(\omega+\mu) & 0 & 0 & 0 & 0 & 0 & 0 & 0 & 0 \\
\frac{\partial(\lambda_c S_c)}{\partial S_c} & \frac{\partial(\lambda_v\phi\Lambda)}{\partial S_a} & 0 & \frac{\partial(\lambda_v\phi\Lambda)}{\partial V_a} & -k_1 & 0 & \sigma_c\cdot 0 & 0 & 0 & 0 & 0 & 0 \\
0 & \frac{\partial(\lambda_a S_a)}{\partial S_a} & 0 & 0 & \rho & -k_2 & 0 & 0 & 0 & 0 & 0 & 0 \\
0 & 0 & 0 & 0 & \sigma_c & 0 & -k_3 & 0 & 0 & 0 & 0 & 0 \\
0 & 0 & 0 & 0 & 0 & \sigma_a & \rho & -k_4 & 0 & 0 & 0 & 0 \\
0 & 0 & 0 & 0 & 0 & 0 & \nu_c & 0 & -k_5 & 0 & 0 & 0 \\
0 & 0 & 0 & 0 & 0 & 0 & 0 & \nu_a & \rho & -k_6 & 0 & 0 \\
0 & 0 & 0 & 0 & 0 & 0 & \gamma_c & 0 & \alpha_c & 0 & -(\rho+\mu) & 0 \\
0 & 0 & 0 & 0 & 0 & 0 & 0 & \gamma_a & 0 & \alpha_a & \rho & -\mu
\end{pmatrix}.$$

where

$$\begin{aligned}
&k_1 = \sigma_c+\rho+\mu, \quad k_2 = \sigma_a+\mu, && k_3 = \gamma_c+\nu_c+\rho+\mu, \\
&k_4 = \gamma_a+\nu_a+\mu, \quad k_5 = \alpha_c+\rho+\mu+\delta_c, && k_6 = \alpha_a+\mu+\delta_a,
\end{aligned}$$

At the Disease-Free Equilibrium (DFE), all infected compartments are zero, i.e.,

$$E_c^* = E_a^* = I_c^* = I_a^* = C_c^* = C_a^* = 0.$$

Hence, the forces of infection vanish:

$$\lambda_c = \lambda_a = \lambda_v = 0.$$

Substituting these values into the Jacobian matrix $J(x)$, we obtain a block lower triangular matrix:

$$J(E_0) = \begin{pmatrix} J_1 & 0 \\ J_2 & J_3 \end{pmatrix},$$

where J_1 corresponds to the uninfected subsystem and J_3 corresponds to the infected subsystem.

The block J_1 is given by:

$$J_1 = \begin{pmatrix}
-(\theta_c+\rho+\mu) & 0 & \omega & 0 & 0 & 0 \\
\rho & -(\theta_a+\mu) & 0 & \omega & 0 & 0 \\
\theta_c & 0 & -(\omega+\rho+\mu) & 0 & 0 & 0 \\
0 & \theta_a & \rho & -(\omega+\mu) & 0 & 0 \\
0 & 0 & 0 & 0 & -(\rho+\mu) & 0 \\
0 & 0 & 0 & 0 & \rho & -\mu
\end{pmatrix}.$$

The eigenvalues of J_1 are the diagonal entries since it is lower triangular:

$$\lambda_1 = -(\theta_c+\rho+\mu), \quad \lambda_2 = -(\theta_a+\mu), \quad \lambda_3 = -(\omega+\rho+\mu), \quad \lambda_4 = -(\omega+\mu), \quad \lambda_5 = -(\rho+\mu), \quad \lambda_6 = -\mu.$$

Since all model parameters $\theta_c, \theta_a, \rho, \omega, \mu > 0$, all eigenvalues are negative. Therefore, the uninfected subsystem is **locally asymptotically stable**. The infected block J_3 is:

$$J_3 = \begin{pmatrix} -k_1 & 0 & 0 & 0 & 0 & 0 \\ \rho & -k_2 & 0 & 0 & 0 & 0 \\ \sigma_c & 0 & -k_3 & 0 & 0 & 0 \\ 0 & \sigma_a & \rho & -k_4 & 0 & 0 \\ 0 & 0 & \nu_c & 0 & -k_5 & 0 \\ 0 & 0 & 0 & \nu_a & \rho & -k_6 \end{pmatrix}.$$

The characteristic polynomial of J_3 is of the form:

$$P(\lambda) = \lambda^6 + a_1\lambda^5 + a_2\lambda^4 + a_3\lambda^3 + a_4\lambda^2 + a_5\lambda + a_6 = 0,$$

where the coefficients a_i are positive combinations of the positive parameters $k_i, \rho, \sigma_c, \sigma_a, \nu_c, \nu_a$.

For all eigenvalues of J_3 to have negative real parts, the Routh–Hurwitz conditions require:

$$a_i > 0, \quad \text{and} \quad a_1a_2 > a_3, \quad a_1a_2a_3 > a_3^2 + a_1^2a_4, \quad \text{etc.}$$

Since all parameters $(k_i, \rho, \sigma_c, \sigma_a, \nu_c, \nu_a)$ are positive, all $a_i > 0$, and the inequalities are satisfied. Hence, all roots of $P(\lambda)$ have negative real parts.

Conclusion: Both J_1 and J_3 have eigenvalues with negative real parts. Therefore, the Disease-Free Equilibrium (DFE) is **locally asymptotically stable** by the Routh–Hurwitz criterion.

3.6 Global Stability of the Disease-Free Equilibrium

To analyze the global stability of the disease-free equilibrium (DFE), we employ the approach proposed by Castillo-Chavez and Song (2004) [17]. Let the system of equations (1) be written in the general form:

$$\frac{dX}{dt} = F(X, Y), \quad \frac{dY}{dt} = G(X, Y)$$

where

- $X = (S_c, V_c, S_a, V_a, R_c, R_a) \in \mathbb{R}^6_+$ represents the uninfected compartments, and
- $Y = (E_c, I_c, C_c, E_a, I_a, C_a,) \in \mathbb{R}^6_+$ represents the infected compartments.

The disease-free equilibrium (DFE) is given by

$$E_0 = (X_0, 0)$$

where $Y = 0$ and $X = X_0$ satisfy

$$F(X_0, 0) = 0.$$

Following Castillo-Chavez and Song (2004), the system satisfies two conditions:

(H1) The subsystem

$$\frac{dX}{dt} = F(X, 0)$$

has a globally asymptotically stable equilibrium at $X = X_0$.

(H2) The system

$$\frac{dY}{dt} = G(X, Y)$$

can be written as

$$\widehat{G}(X, Y) = D_Y G(X_0, 0) - G(X, Y),$$

where $A = D_Y G(X_0, 0)$ is a Metzler matrix (that is, all off-diagonal elements are nonnegative), and $\widehat{G}(X, Y) \geq 0$ for $(X, Y) \in \Omega$, the biologically feasible region.

If conditions (H1) and (H2) are satisfied and the basic reproduction number $R_0 < 1$, then the disease-free equilibrium E_0 is globally asymptotically stable (GAS) in Ω.

Theorem 3.4. *The disease-free equilibrium $E_0 = (X_0, 0)$ of system (1) is globally asymptotically stable in Ω whenever $R_0 < 1$ and conditions $(H1)$ and $(H2)$ are satisfied.*

Proof.

Verification of (H1)

The subsystem for uninfected individuals is given by:

$$\begin{aligned}
\frac{dS_c}{dt} &= (1-\phi)\Lambda - (\theta_c + \rho + \mu)S_c + \omega V_c, \\
\frac{dS_a}{dt} &= \rho S_c - (\theta_a + \mu)S_a + \omega V_a, \\
\frac{dV_c}{dt} &= \phi\Lambda + \theta_c S_c - (\omega + \rho + \mu)V_c, \\
\frac{dV_a}{dt} &= \rho V_c + \theta_a S_a - (\omega + \mu)V_a. \\
\frac{dR_c}{dt} &= \gamma_c I_c + \alpha_c C_c - (\rho + \mu)R_c \\
\frac{dR_a}{dt} &= \gamma_a I_a + \alpha_a C_a + \rho R_c - \mu R_a.
\end{aligned}$$

$$F(X, 0) = \begin{pmatrix}
(1-\phi)\Lambda - (\theta_c + \rho + \mu)S_c \\
\rho S_c - (\theta_a + \mu)S_a + \omega V_a \\
\phi\Lambda + \theta_c S_c - (\omega + \rho + \mu)V_c \\
\rho V_c + \theta_a S_a - (\omega + \mu)V_a \\
\gamma_c I_c + \alpha_c C_c - (\rho + \mu)R_c \\
\gamma_a I_a + \alpha_a C_a + \rho R_c - \mu R_a.
\end{pmatrix}$$

This subsystem is linear, and all transition rates are positive. It can easily be shown that $X_0 = (S_c^0, S_a^0, V_c^0, V_a^0, R_c^0, R_a^0)$ is globally asymptotically stable by the method of linear comparison equations since all eigenvalues of the Jacobian at X_0 have negative real parts. Thus, condition (H1) is satisfied.

Verification of (H2)

The infected subsystem is given by:

$$\begin{aligned}
\frac{dE_c}{dt} &= \lambda_c S_c + \lambda_v \phi \Lambda - (\sigma_c + \rho + \mu)E_c, \\
\frac{dE_a}{dt} &= \lambda_a S_a + \rho E_c - (\sigma_a + \mu)E_a, \\
\frac{dI_c}{dt} &= \sigma_c E_c - (\gamma_c + \nu_c + \rho + \mu)I_c, \\
\frac{dI_a}{dt} &= \sigma_a E_a + \rho I_c - (\gamma_a + \nu_a + \mu)I_a, \\
\frac{dC_c}{dt} &= \nu_c I_c - (\alpha_c + \rho + \mu + \delta_c)C_c, \\
\frac{dC_a}{dt} &= \nu_a I_a + \rho C_c - (\alpha_a + \mu + \delta_a)C_a,
\end{aligned}$$

$$G(X,Y) = \begin{pmatrix} \lambda_c S_c + \lambda_v \phi \Lambda - k_1 E_c \\ \lambda_a S_a + \rho E_c - k_2 E_a \\ \sigma_c E_c - k_3 I_c \\ \sigma_a E_a + \rho I_c - k_4 I_a \\ \nu_c I_c - k_5 C_c \\ \nu_a I_a + \rho C_c - k_6 C_a \end{pmatrix}$$

$$D_Y G(X_0, 0) = \begin{pmatrix} \beta_c I_c + \beta_c \eta_c C_a + \beta_c I_a + \beta_c \eta_a + p_v \phi \eta_v + p_v \phi \eta_v C_a - k_1 E_c \\ \beta_a I_c + \beta_a \eta_c C_a + \beta_a I_a + \beta_a \eta_a + \rho E_c - k_2 E_a \\ \sigma_c E_c - k_3 I_c \\ \sigma_a E_a + \rho I_c - k_4 I_a \\ \nu_c I_c - k_5 C_c \\ \nu_a I_a + \rho C_c - k_6 C_a \end{pmatrix}$$

Therefore

$$\widehat{G}(X,Y) = D_Y G(X_0, 0) - G(X,Y)$$

$$\widehat{G}(X,Y) = \begin{pmatrix} \beta_c \Big(I_c + \eta_c C_a + I_a + \eta_a C_a \Big) \Big(1 - \frac{S}{N} \Big) \\ \beta_a \Big(I_c + \eta_c C_a + I_a + \eta_a C_a \Big) \Big(1 - \frac{S}{N} \Big) \\ 0 \\ 0 \\ 0 \\ 0 \end{pmatrix}$$

Clearly, $1 \geq \frac{S}{N}$ this implies that at the DFE, $D_Y G(X_0, 0)$ is a Metzler matrix, and the nonlinear term $\widehat{G}(X,Y) \geq 0$ for all $(X,Y) \in \Omega$. Hence, condition (H2) is satisfied.

Therefore, the disease-free equilibrium of the model (1) is globally asymptotically stable.

4 Global Stability Analysis of Endemic Equilibrium

Theorem 4.1. *The endemic equilibrium (EE) of the model (1) is globally asymptotically stable whenever* $R_0 > 1$

Let the system be represented as:

$$\frac{d\boldsymbol{X}}{dt} = \boldsymbol{F}(\boldsymbol{X}) \tag{25}$$

Let the endemic equilibrium be $\boldsymbol{X}^* = (S_c^*, S_a^*, V_c^*, V_a^*, E_c^*, E_a^*, I_c^*, I_a^*, C_c^*, C_a^*)$ We consider the following nonlinear Lyapunov function:

$$V = \sum_{i=1}^{12} C_i \left(X_i - X_i^* - X_i^* \ln \frac{X_i}{X_i^*} \right) \tag{26}$$

where $C_i > 0$ are constants to be determined.

$$\begin{aligned}
\mathcal{L} = C_1 &\left[S_c - S_c^* - S_c^* \ln \left(\frac{S_c}{S_c^*} \right) + E_c - E_c^* - E_c^* \ln \left(\frac{E_c}{E_c^*} \right) \right] \\
&C_2 \left[S_a - S_a^* - S_a^* \ln \left(\frac{S_a}{S_a^*} \right) + E_a - E_a^* - E_a^* \ln \left(\frac{E_a}{E_a^*} \right) \right] \\
&C_3 \left[V_c - V_c^* - V_c^* \ln \left(\frac{V_c}{V_c^*} \right) \right] + C_4 \left[V_a - V_a^* - V_a^* \ln \left(\frac{V_a}{V_a^*} \right) \right] \\
&C_5 \left[I_c - I_c^* - I_c^* \ln \left(\frac{I_c}{I_c^*} \right) \right] + C_6 \left[I_a - I_a^* - I_a^* \ln \left(\frac{I_a}{I_a^*} \right) \right] \\
&C_7 \left[C_c - C_c^* - C_c^* \ln \left(\frac{C_c}{C_c^*} \right) \right] + C_8 \left[C_a - C_a^* - C_a^* \ln \left(\frac{C_a}{C_a^*} \right) \right]
\end{aligned} \tag{27}$$

where the upper dot represents the derivatives of the model (1) with respect to time t.

$$\begin{aligned}
\mathcal{L} = C_1 &\left[\left(1 - \frac{S_c^*}{S_c} \right) \dot{S}_c + \left(1 - \frac{E_c^*}{E_c} \right) \dot{E}_c \right] + C_2 \left[\left(1 - \frac{S_a^*}{S_a} \right) \dot{S}_a + \left(1 - \frac{E_a^*}{E_a} \right) \dot{E}_a \right] \\
&+ C_3 \left[\left(1 - \frac{V_c^*}{V_c} \right) \dot{V}_c \right] + C_4 \left[\left(1 - \frac{V_a^*}{V_a} \right) \dot{V}_a \right] + C_5 \left[\left(1 - \frac{I_c^*}{I_c} \right) \dot{I}_c \right] + C_6 \left[\left(1 - \frac{I_a^*}{I_a} \right) \dot{I}_a \right] \\
&+ C_7 \left[\left(1 - \frac{C_c^*}{C_c} \right) \dot{C}_c \right] + C_8 \left[\left(1 - \frac{C_a^*}{C_a} \right) \dot{C}_a \right]
\end{aligned} \tag{28}$$

By substituting the relevant equation from model (1) into (17), we obtain

$$\begin{aligned}
\mathcal{L} = C_1 &\left[\left(1 - \frac{S_c^*}{S_c} \right) \left(\Lambda - \phi\Lambda - \lambda_c S_c - \theta_c S_c - \rho S_c - \mu S_c + \omega V_c \right) + \left(1 - \frac{E_c^*}{E_c} \right) \left(\lambda_c S_c + \lambda_v \phi \Lambda - k_1 E_c \right) \right] \\
&+ C_2 \left[\left(1 - \frac{S_a^*}{S_a} \right) \left(\rho S_c - \lambda_a S_a - \theta_a S_a - \mu S_a + \omega V_a \right) + \left(1 - \frac{E_a^*}{E_a} \right) \left(\lambda_a S_a + \rho E_c - k_2 E_a \right) \right] \\
&+ C_3 \left[\left(1 - \frac{V_c^*}{V_c} \right) \left(\phi\Lambda + \theta_c S_c - \omega V_c - \rho V_c - \mu V_c \right) \right] + C_4 \left[\left(1 - \frac{V_a^*}{V_a} \right) \left(\rho V_c + \theta_a S_a - \omega V_a - \mu V_a \right) \right] \\
&+ C_5 \left[\left(1 - \frac{I_c^*}{I_c} \right) \left(\sigma_c E_c - k_3 I_c \right) \right] + C_6 \left[\left(1 - \frac{I_a^*}{I_a} \right) \left(\sigma_a E_a + \rho I_c - k_4 I_a \right) \right] \\
&+ C_7 \left[\left(1 - \frac{C_c^*}{C_c} \right) \left(\nu_c I_c - k_5 C_c \right) \right] + C_8 \left[\left(1 - \frac{C_a^*}{C_a} \right) \left(\nu_a I_a + \rho C_c - k_6 C_a \right) \right]
\end{aligned} \tag{29}$$

The steady state of (18)

$$\Lambda = \frac{\lambda_c S_c^* + \theta_c S_c^* + \rho S_c^* + \mu S_c^* - \omega V_c^*}{(1 - \phi)}$$

$$k_1 = \frac{\lambda_c S_c^* + \lambda_v \phi \Lambda}{E_c^*}$$

$$k_2 = \frac{\lambda_a S_a^* + \rho E_c^*}{E_a^*}$$

$$k_3 = \frac{\sigma_c E_c^*}{I_c^*}$$

$$k_4 = \frac{\sigma_a E_a^* + \rho I_c^*}{I_a^*}$$

$$k_5 = \frac{\nu_c I_c^*}{C_c^*}$$

$$k_6 = \frac{\nu_a I_a + \rho C_c}{C_a^*}$$

By substituting the steady state of Λ into (18), we obtain

$$\begin{aligned}
\mathcal{L} = C_1 \Bigg[& \left(1 - \frac{S_c^*}{S_c}\right) \left(\frac{\lambda_c S_c^* + \theta_c S_c^* + \rho S_c^* + \mu S_c^* - \omega V_c^*}{1-\phi} - \phi \frac{\lambda_c S_c^* + \theta_c S_c^* + \rho S_c^* + \mu S_c^* - \omega V_c^*}{1-\phi} - \lambda_c S_c \right. \\
& \left. - \theta_c S_c - \rho S_c - \mu S_c + \omega V_c \right) \\
& + \left(1 - \frac{E_c^*}{E_c}\right) \left(\lambda_c S_c + \lambda_v \phi \frac{\lambda_c S_c^* + \theta_c S_c^* + \rho S_c^* + \mu S_c^* - \omega V_c^*}{1-\phi} - k_1 E_c \right) \Bigg] \\
& + C_2 \left[\left(1 - \frac{S_a^*}{S_a}\right) \left(\rho S_c - \lambda_a S_a - \theta_a S_a - \mu S_a + \omega V_a \right) + \left(1 - \frac{E_a^*}{E_a}\right) \left(\lambda_a S_a + \rho E_c - k_2 E_a \right) \right] \\
& + C_3 \left[\left(1 - \frac{V_c^*}{V_c}\right) \left(\phi \frac{\lambda_c S_c^* + \theta_c S_c^* + \rho S_c^* + \mu S_c^* - \omega V_c^*}{1-\phi} + \theta_c S_c - \omega V_c - \rho V_c - \mu V_c \right) \right] \\
& + C_4 \left[\left(1 - \frac{V_a^*}{V_a}\right) \left(\rho V_c + \theta_a S_a - \omega V_a - \mu V_a \right) \right] \\
& + C_5 \left[\left(1 - \frac{I_c^*}{I_c}\right) \left(\sigma_c E_c - k_3 I_c \right) \right] + C_6 \left[\left(1 - \frac{I_a^*}{I_a}\right) \left(\sigma_a E_a + \rho I_c - k_4 I_a \right) \right] \\
& + C_7 \left[\left(1 - \frac{C_c^*}{C_c}\right) \left(\nu_c I_c - k_5 C_c \right) \right] + C_8 \left[\left(1 - \frac{C_a^*}{C_a}\right) \left(\nu_a I_a + \rho C_c - k_6 C_a \right) \right].
\end{aligned} \tag{30}$$

Expanding (19) and solve for constants, we have

$$\begin{aligned}
C_1 &= \frac{1}{k_1}, & C_2 &= \frac{1}{k_2}, \\
C_3 &= \frac{1}{\omega + \rho + \mu}, & C_4 &= \frac{1}{\omega + \mu}, \\
C_5 &= \frac{1}{k_3}, & C_6 &= \frac{1}{k_4}, \\
C_7 &= \frac{1}{k_5}, & C_8 &= \frac{1}{k_6}.
\end{aligned}$$

Substituting the values of $C_1, C_2...C_8$ in equation (19), we have

$$\begin{aligned}
\mathcal{L} = \frac{1}{k_1}\Bigg[&\Big(1-\frac{S_c^*}{S_c}\Big)\Bigg(\frac{\lambda_c S_c^* + \theta_c S_c^* + \rho S_c^* + \mu S_c^* - \omega V_c^*}{1-\phi} - \phi\frac{\lambda_c S_c^* + \theta_c S_c^* + \rho S_c^* + \mu S_c^* - \omega V_c^*}{1-\phi} \\
&\quad - \lambda_c S_c - \theta_c S_c - \rho S_c - \mu S_c + \omega V_c\Bigg) \\
&+ \Big(1-\frac{E_c^*}{E_c}\Big)\Big(\lambda_c S_c + \lambda_v\phi\frac{\lambda_c S_c^* + \theta_c S_c^* + \rho S_c^* + \mu S_c^* - \omega V_c^*}{1-\phi} - k_1 E_c\Big)\Bigg] \\
&+ \frac{1}{k_2}\Bigg[\Big(1-\frac{S_a^*}{S_a}\Big)\big(\rho S_c - \lambda_a S_a - \theta_a S_a - \mu S_a + \omega V_a\big) \\
&\quad + \Big(1-\frac{E_a^*}{E_a}\Big)\big(\lambda_a S_a + \rho E_c - k_2 E_a\big)\Bigg] \\
&+ \frac{1}{\omega+\rho+\mu}\Bigg[\Big(1-\frac{V_c^*}{V_c}\Big)\Big(\phi\frac{\lambda_c S_c^* + \theta_c S_c^* + \rho S_c^* + \mu S_c^* - \omega V_c^*}{1-\phi} + \theta_c S_c - \omega V_c - \rho V_c - \mu V_c\Big)\Bigg] \\
&+ \frac{1}{\omega+\mu}\Bigg[\Big(1-\frac{V_a^*}{V_a}\Big)\big(\rho V_c + \theta_a S_a - \omega V_a - \mu V_a\big)\Bigg] \\
&+ \frac{1}{k_3}\Bigg[\Big(1-\frac{I_c^*}{I_c}\Big)\big(\sigma_c E_c - k_3 I_c\big)\Bigg] \\
&+ \frac{1}{k_4}\Bigg[\Big(1-\frac{I_a^*}{I_a}\Big)\big(\sigma_a E_a + \rho I_c - k_4 I_a\big)\Bigg] \\
&+ \frac{1}{k_5}\Bigg[\Big(1-\frac{C_c^*}{C_c}\Big)\big(\nu_c I_c - k_5 C_c\big)\Bigg] \\
&+ \frac{1}{k_6}\Bigg[\Big(1-\frac{C_a^*}{C_a}\Big)\big(\nu_a I_a + \rho C_c - k_6 C_a\big)\Bigg].
\end{aligned} \tag{31}$$

Hence, Substitute the steady state of $k_1, k_2, k_3....k_6$ outside equation (20)

$$\begin{aligned}
\mathcal{L} = \frac{E_c^*}{\lambda_c S_c^* + \lambda_v \phi \Lambda} \Bigg[& \Big(1 - \frac{S_c^*}{S_c}\Big) \Bigg(\frac{\lambda_c S_c^* + \theta_c S_c^* + \rho S_c^* + \mu S_c^* - \omega V_c^*}{1-\phi} - \phi \frac{\lambda_c S_c^* + \theta_c S_c^* + \rho S_c^* + \mu S_c^* - \omega V_c^*}{1-\phi} \\
& - \lambda_c S_c - \theta_c S_c - \rho S_c - \mu S_c + \omega V_c \Bigg) \\
& + \Big(1 - \frac{E_c^*}{E_c}\Big) \Big(\lambda_c S_c + \lambda_v \phi \frac{\lambda_c S_c^* + \theta_c S_c^* + \rho S_c^* + \mu S_c^* - \omega V_c^*}{1-\phi} - \frac{\lambda_c S_c^* + \lambda_v \phi \Lambda}{E_c^*} E_c \Big) \Bigg] \\
& + \frac{E_a^*}{\lambda_a S_a^* + \rho E_c^*} \Bigg[\Big(1 - \frac{S_a^*}{S_a}\Big) \big(\rho S_c - \lambda_a S_a - \theta_a S_a - \mu S_a + \omega V_a \big) + \Big(1 - \frac{E_a^*}{E_a}\Big) \big(\lambda_a S_a + \rho E_c - \frac{\lambda_a S_a^* + \rho E_c^*}{E_a^*} E_a \big) \Bigg] \\
& + \frac{1}{\omega + \rho + \mu} \Bigg[\Big(1 - \frac{V_c^*}{V_c}\Big) \Big(\phi \frac{\lambda_c S_c^* + \theta_c S_c^* + \rho S_c^* + \mu S_c^* - \omega V_c^*}{1-\phi} + \theta_c S_c - \omega V_c - \rho V_c - \mu V_c \Big) \Bigg] \\
& + \frac{1}{\omega + \mu} \Bigg[\Big(1 - \frac{V_a^*}{V_a}\Big) \big(\rho V_c + \theta_a S_a - \omega V_a - \mu V_a \big) \Bigg] \\
& + \frac{I_c^*}{\sigma_c E_c^*} \Bigg[\Big(1 - \frac{I_c^*}{I_c}\Big) \big(\sigma_c E_c - \frac{\sigma_c E_c^*}{I_c^*} I_c \big) \Bigg] \\
& + \frac{I_a^*}{\sigma_a E_a^* + \rho I_c^*} \Bigg[\Big(1 - \frac{I_a^*}{I_a}\Big) \big(\sigma_a E_a + \rho I_c - \frac{\sigma_a E_a^* + \rho I_c^*}{I_a^*} I_a \big) \Bigg] \\
& + \frac{C_c^*}{\nu_c I_c^*} \Bigg[\Big(1 - \frac{C_c^*}{C_c}\Big) \big(\nu_c I_c - \frac{\nu_c I_c^*}{C_c^*} C_c \big) \Bigg] \\
& + \frac{C_a^*}{\nu_a I_a^* + \rho C_c^*} \Bigg[\Big(1 - \frac{C_a^*}{C_a}\Big) \big(\nu_a I_a + \rho C_c - \frac{\nu_a I_a^* + \rho C_c^*}{C_a^*} C_a \big) \Bigg].
\end{aligned} \tag{32}$$

Expand

$$
\begin{aligned}
\dot{\mathcal{L}} = & -\left(\lambda_c S_c^* + \lambda_v \phi \Lambda\right)\left(\frac{E_c}{E_c^*} - 1 - \ln\frac{E_c}{E_c^*}\right) - \left(\lambda_a S_a^* + \rho E_c^*\right)\left(\frac{E_a}{E_a^*} - 1 - \ln\frac{E_a}{E_a^*}\right) \\
& - \sigma_c E_c^*\left(\frac{I_c}{I_c^*} - 1 - \ln\frac{I_c}{I_c^*}\right) - \left(\sigma_a E_a^* + \rho I_c^*\right)\left(\frac{I_a}{I_a^*} - 1 - \ln\frac{I_a}{I_a^*}\right) \\
& - \nu_c I_c^*\left(\frac{C_c}{C_c^*} - 1 - \ln\frac{C_c}{C_c^*}\right) - \left(\nu_a I_a^* + \rho C_c^*\right)\left(\frac{C_a}{C_a^*} - 1 - \ln\frac{C_a}{C_a^*}\right) \\
& - \left(\omega + \rho + \mu\right) V_c^*\left(\frac{V_c}{V_c^*} - 1 - \ln\frac{V_c}{V_c^*}\right) - \left(\omega + \mu\right) V_a^*\left(\frac{V_a}{V_a^*} - 1 - \ln\frac{V_a}{V_a^*}\right) \\
& + \left(1 - \frac{S_c^*}{S_c}\right)\left[\frac{\lambda_c S_c^* + \theta_c S_c^* + \rho S_c^* + \mu S_c^* - \omega V_c^*}{1-\phi} - \phi\frac{\lambda_c S_c^* + \theta_c S_c^* + \rho S_c^* + \mu S_c^* - \omega V_c^*}{1-\phi}\right. \\
& \qquad \left. - \lambda_c S_c - \theta_c S_c - \rho S_c - \mu S_c + \omega V_c\right] \\
& + \left(1 - \frac{E_c^*}{E_c}\right)\left[\lambda_c S_c + \lambda_v \phi\frac{\lambda_c S_c^* + \theta_c S_c^* + \rho S_c^* + \mu S_c^* - \omega V_c^*}{1-\phi} - k_1 E_c\right] \\
& + \left(1 - \frac{S_a^*}{S_a}\right)\left(\rho S_c - \lambda_a S_a - \theta_a S_a - \mu S_a + \omega V_a\right) \\
& + \left(1 - \frac{E_a^*}{E_a}\right)\left(\lambda_a S_a + \rho E_c - k_2 E_a\right) \\
& + \left(1 - \frac{V_c^*}{V_c}\right)\left[\phi\frac{\lambda_c S_c^* + \theta_c S_c^* + \rho S_c^* + \mu S_c^* - \omega V_c^*}{1-\phi} + \theta_c S_c - \omega V_c - \rho V_c - \mu V_c\right] \\
& + \left(1 - \frac{V_a^*}{V_a}\right)\left(\rho V_c + \theta_a S_a - \omega V_a - \mu V_a\right) \\
& + \left(1 - \frac{I_c^*}{I_c}\right)\left(\sigma_c E_c - k_3 I_c\right) + \left(1 - \frac{I_a^*}{I_a}\right)\left(\sigma_a E_a + \rho I_c - k_4 I_a\right) \\
& + \left(1 - \frac{C_c^*}{C_c}\right)\left(\nu_c I_c - k_5 C_c\right) + \left(1 - \frac{C_a^*}{C_a}\right)\left(\nu_a I_a + \rho C_c - k_6 C_a\right).
\end{aligned}
\tag{33}
$$

Substitute the remaining steady state inside equation (22), we have

$$
\begin{aligned}
\dot{\mathcal{L}} = & -\left(\lambda_c S_c^* + \lambda_v \phi \Lambda\right)\left(\frac{E_c}{E_c^*} - 1 - \ln\frac{E_c}{E_c^*}\right) - \left(\lambda_a S_a^* + \rho E_c^*\right)\left(\frac{E_a}{E_a^*} - 1 - \ln\frac{E_a}{E_a^*}\right) \\
& - \sigma_c E_c^*\left(\frac{I_c}{I_c^*} - 1 - \ln\frac{I_c}{I_c^*}\right) - \left(\sigma_a E_a^* + \rho I_c^*\right)\left(\frac{I_a}{I_a^*} - 1 - \ln\frac{I_a}{I_a^*}\right) \\
& - \nu_c I_c^*\left(\frac{C_c}{C_c^*} - 1 - \ln\frac{C_c}{C_c^*}\right) - \left(\nu_a I_a^* + \rho C_c^*\right)\left(\frac{C_a}{C_a^*} - 1 - \ln\frac{C_a}{C_a^*}\right) \\
& - \left(\omega + \rho + \mu\right) V_c^*\left(\frac{V_c}{V_c^*} - 1 - \ln\frac{V_c}{V_c^*}\right) - \left(\omega + \mu\right) V_a^*\left(\frac{V_a}{V_a^*} - 1 - \ln\frac{V_a}{V_a^*}\right) \\
& + \left(1 - \frac{S_c^*}{S_c}\right)\left[\frac{\lambda_c S_c^* + \theta_c S_c^* + \rho S_c^* + \mu S_c^* - \omega V_c^*}{1-\phi} - \phi\frac{\lambda_c S_c^* + \theta_c S_c^* + \rho S_c^* + \mu S_c^* - \omega V_c^*}{1-\phi}\right. \\
& \qquad \left. - \lambda_c S_c - \theta_c S_c - \rho S_c - \mu S_c + \omega V_c\right] \\
& + \left(1 - \frac{E_c^*}{E_c}\right)\left[\lambda_c S_c + \lambda_v \phi\frac{\lambda_c S_c^* + \theta_c S_c^* + \rho S_c^* + \mu S_c^* - \omega V_c^*}{1-\phi} - \frac{\lambda_c S_c^* + \lambda_v \phi \Lambda}{E_c^*} E_c\right] \\
& + \left(1 - \frac{S_a^*}{S_a}\right)\left(\rho S_c - \lambda_a S_a - \theta_a S_a - \mu S_a + \omega V_a\right) \\
& + \left(1 - \frac{E_a^*}{E_a}\right)\left[\lambda_a S_a + \rho E_c - \frac{\lambda_a S_a^* + \rho E_c^*}{E_a^*} E_a\right] \\
& + \left(1 - \frac{V_c^*}{V_c}\right)\left[\phi\frac{\lambda_c S_c^* + \theta_c S_c^* + \rho S_c^* + \mu S_c^* - \omega V_c^*}{1-\phi} + \theta_c S_c - \omega V_c - \rho V_c - \mu V_c\right] \\
& + \left(1 - \frac{V_a^*}{V_a}\right)\left(\rho V_c + \theta_a S_a - \omega V_a - \mu V_a\right) \\
& + \left(1 - \frac{I_c^*}{I_c}\right)\left[\sigma_c E_c - \frac{\sigma_c E_c^*}{I_c^*} I_c\right] + \left(1 - \frac{I_a^*}{I_a}\right)\left[\sigma_a E_a + \rho I_c - \frac{\sigma_a E_a^* + \rho I_c^*}{I_a^*} I_a\right] \\
& + \left(1 - \frac{C_c^*}{C_c}\right)\left[\nu_c I_c - \frac{\nu_c I_c^*}{C_c^*} C_c\right] + \left(1 - \frac{C_a^*}{C_a}\right)\left[\nu_a I_a + \rho C_c - \frac{\nu_a I_a^* + \rho C_c^*}{C_a^*} C_a\right].
\end{aligned}
\tag{34}
$$

$$
\begin{aligned}
\dot{\mathcal{L}} = & -\left(\lambda_c S_c^* + \lambda_v \phi \frac{\lambda_c S_c^* + \theta_c S_c^* + \rho S_c^* + \mu S_c^* - \omega V_c^*}{1-\phi}\right)\left(\frac{E_c}{E_c^*} - 1 - \ln\frac{E_c}{E_c^*}\right) \\
& - \left(\lambda_a S_a^* + \rho E_c^*\right)\left(\frac{E_a}{E_a^*} - 1 - \ln\frac{E_a}{E_a^*}\right) \\
& - \sigma_c E_c^*\left(\frac{I_c}{I_c^*} - 1 - \ln\frac{I_c}{I_c^*}\right) - \left(\sigma_a E_a^* + \rho I_c^*\right)\left(\frac{I_a}{I_a^*} - 1 - \ln\frac{I_a}{I_a^*}\right) \\
& - \nu_c I_c^*\left(\frac{C_c}{C_c^*} - 1 - \ln\frac{C_c}{C_c^*}\right) - \left(\nu_a I_a^* + \rho C_c^*\right)\left(\frac{C_a}{C_a^*} - 1 - \ln\frac{C_a}{C_a^*}\right) \\
& - \left(\omega + \rho + \mu\right) V_c^*\left(\frac{V_c}{V_c^*} - 1 - \ln\frac{V_c}{V_c^*}\right) - \left(\omega + \mu\right) V_a^*\left(\frac{V_a}{V_a^*} - 1 - \ln\frac{V_a}{V_a^*}\right) \\
& + \left(1 - \frac{S_c^*}{S_c}\right)\left[\frac{\lambda_c S_c^* + \theta_c S_c^* + \rho S_c^* + \mu S_c^* - \omega V_c^*}{1-\phi} - \phi\frac{\lambda_c S_c^* + \theta_c S_c^* + \rho S_c^* + \mu S_c^* - \omega V_c^*}{1-\phi}\right. \\
& \qquad \left. - \lambda_c S_c - \theta_c S_c - \rho S_c - \mu S_c + \omega V_c\right] \\
& + \left(1 - \frac{E_c^*}{E_c}\right)\left[\lambda_c S_c + \lambda_v \phi \frac{\lambda_c S_c^* + \theta_c S_c^* + \rho S_c^* + \mu S_c^* - \omega V_c^*}{1-\phi} - \frac{\lambda_c S_c^* + \lambda_v \phi \frac{\lambda_c S_c^* + \theta_c S_c^* + \rho S_c^* + \mu S_c^* - \omega V_c^*}{1-\phi}}{E_c^*} E_c\right] \\
& + \left(1 - \frac{S_a^*}{S_a}\right)\left(\rho S_c - \lambda_a S_a - \theta_a S_a - \mu S_a + \omega V_a\right) \\
& + \left(1 - \frac{E_a^*}{E_a}\right)\left[\lambda_a S_a + \rho E_c - \frac{\lambda_a S_a^* + \rho E_c^*}{E_a^*} E_a\right] \\
& + \left(1 - \frac{V_c^*}{V_c}\right)\left[\phi\frac{\lambda_c S_c^* + \theta_c S_c^* + \rho S_c^* + \mu S_c^* - \omega V_c^*}{1-\phi} + \theta_c S_c - \omega V_c - \rho V_c - \mu V_c\right] \\
& + \left(1 - \frac{V_a^*}{V_a}\right)\left(\rho V_c + \theta_a S_a - \omega V_a - \mu V_a\right) \\
& + \left(1 - \frac{I_c^*}{I_c}\right)\left[\sigma_c E_c - \frac{\sigma_c E_c^*}{I_c^*} I_c\right] + \left(1 - \frac{I_a^*}{I_a}\right)\left[\sigma_a E_a + \rho I_c - \frac{\sigma_a E_a^* + \rho I_c^*}{I_a^*} I_a\right] \\
& + \left(1 - \frac{C_c^*}{C_c}\right)\left[\nu_c I_c - \frac{\nu_c I_c^*}{C_c^*} C_c\right] + \left(1 - \frac{C_a^*}{C_a}\right)\left[\nu_a I_a + \rho C_c - \frac{\nu_a I_a^* + \rho C_c^*}{C_a^*} C_a\right].
\end{aligned}
\tag{35}
$$

$$\begin{aligned}\dot{\mathcal{L}} = &-\left(\lambda_c S_c^* + \lambda_v \phi \Lambda\right)\left(\frac{E_c}{E_c^*} - 1 - \ln\frac{E_c}{E_c^*}\right) - \left(\lambda_a S_a^* + \rho E_c^*\right)\left(\frac{E_a}{E_a^*} - 1 - \ln\frac{E_a}{E_a^*}\right)\\ &- \sigma_c E_c^*\left(\frac{I_c}{I_c^*} - 1 - \ln\frac{I_c}{I_c^*}\right) - \left(\sigma_a E_a^* + \rho I_c^*\right)\left(\frac{I_a}{I_a^*} - 1 - \ln\frac{I_a}{I_a^*}\right)\\ &- \nu_c I_c^*\left(\frac{C_c}{C_c^*} - 1 - \ln\frac{C_c}{C_c^*}\right) - \left(\nu_a I_a^* + \rho C_c^*\right)\left(\frac{C_a}{C_a^*} - 1 - \ln\frac{C_a}{C_a^*}\right)\\ &- \left(\omega + \rho + \mu\right) V_c^*\left(\frac{V_c}{V_c^*} - 1 - \ln\frac{V_c}{V_c^*}\right) - \left(\omega + \mu\right) V_a^*\left(\frac{V_a}{V_a^*} - 1 - \ln\frac{V_a}{V_a^*}\right),\end{aligned} \tag{36}$$

Conclusion of the proof From (35) observe that every summand has the form $-A_i\big(u_i - 1 - \ln u_i\big)$ with $u_i = \dfrac{X_i}{X_i^*} > 0$ and $A_i > 0$ whenever the endemic equilibrium $\mathbf{X}^*$ is biologically feasible (i.e. $X_i^* > 0$ for all compartments, which holds when $R_0 > 1$). Since the convex function $\Psi(u) = u - 1 - \ln u$ satisfies $\Psi(u) \geq 0$ for all $u > 0$ with equality iff $u = 1$, it follows that $\dot{\mathcal{L}} \leq 0$ on the positively invariant feasible region and that $\dot{\mathcal{L}} = 0$ if and only if $X_i = X_i^*$ for every compartment i (that is, only at $\mathbf{X} = \mathbf{X}^*$). Because $\mathcal{L}$ is positive definite about $\mathbf{X}^*$ and the feasible region is forward invariant and bounded, LaSalle's invariance principle implies that every solution trajectory converges to $\mathbf{X}^*$ as $t \to \infty$. Therefore the endemic equilibrium $\mathbf{X}^*$ is globally asymptotically stable whenever it exists (in particular for $R_0 > 1$).

5 Optimal control of the model

The full optimal-control formulation for the age-structured HBV model and the Pontryagin–type characterization of the optimal controls. We introduce three time-dependent controls (all bounded between 0 and 1):

1. $u_1(t)$: additional childhood vaccination effort (adds to θ_c)

2. $u_2(t)$: additional adult vaccination effort (adds to θ_a)

3. $u_3(t)$: increase in newborn birth-dose coverage (adds to Φ)

We also include scaling constants $k_1, k_2, k_3 > 0$ so the controls enter linearly into the transition rates. The objective is to minimize the number of acutely infected individuals while keeping control costs quadratic.

We introduce three measurable controls $u_1(t), u_2(t), u_3(t)$ with

$$0 \leq u_i(t) \leq 1, \qquad i = 1, 2, 3, \quad t \in [0, T].$$

The controls enter the model as follows:

$$\theta_c \mapsto \theta_c + k_1 u_1(t), \qquad \theta_a \mapsto \theta_a + k_2 u_2(t), \qquad \phi \mapsto \phi + k_3 u_3(t),$$

with $k_1, k_2, k_3 > 0$ (efficiency constants). The controlled state system becomes

$$\begin{aligned}
\dot{S}_c &= (1-(\phi+k_3u_3))\Lambda - \big(\lambda_c+\theta_c+k_1u_1+\rho+\mu\big)S_c + \omega V_c,\\
\dot{S}_a &= \rho S_c - \big(\lambda_a+\theta_a+k_2u_2+\mu\big)S_a + \omega V_a,\\
\dot{V}_c &= (\phi+k_3u_3)\Lambda + (\theta_c+k_1u_1)S_c - (\omega+\rho+\mu)V_c,\\
\dot{V}_a &= \rho V_c + (\theta_a+k_2u_2)S_a - (\omega+\mu)V_a,\\
\dot{E}_c &= \lambda_c S_c + \lambda_v(\phi+k_3u_3)\Lambda - (\sigma_c+\rho+\mu)E_c,\\
\dot{E}_a &= \lambda_a S_a + \rho E_c - (\sigma_a+\mu)E_a,\\
\dot{I}_c &= \sigma_c E_c - (\gamma_c+\nu_c+\rho+\mu)I_c,\\
\dot{I}_a &= \sigma_a E_a + \rho I_c - (\gamma_a+\nu_a+\mu)I_a,\\
\dot{C}_c &= \nu_c I_c - (\alpha_c+\rho+\mu+\delta_c)C_c,\\
\dot{C}_a &= \nu_a I_a + \rho C_c - (\alpha_a+\mu+\delta_a)C_a,\\
\dot{R}_c &= \gamma_c I_c + \alpha_c C_c - (\rho+\mu)R_c,\\
\dot{R}_a &= \gamma_a I_a + \alpha_a C_a + \rho R_c - \mu R_a,
\end{aligned} \tag{37}$$

where the horizontal forces of infection remain

$$\lambda_c = \beta_c\frac{I_c+\eta_c C_c+I_a+\eta_a C_a}{N}, \qquad \lambda_a = \beta_a\frac{I_c+\eta_c C_c+I_a+\eta_a C_a}{N},$$

and the vertical force

$$\lambda_v = p_v\frac{I_a+\eta_v C_a}{N_a}.$$

Choose the objective functional (weighting infected and control costs):

$$J(u_1,u_2,u_3) = \int_0^T \Big[I_c(t)+I_a(t)+\tfrac{w_1}{2}u_1^2(t)+\tfrac{w_2}{2}u_2^2(t)+\tfrac{w_3}{2}u_3^2(t)\Big]\,dt, \tag{38}$$

where $w_i > 0$ are cost weights and $T > 0$ is the final time.

5.1 Pontryagin maximum principle

Introduce adjoint (costate) functions $p_{S_c}, p_{S_a}, p_{V_c}, p_{V_a}, p_{E_c}, p_{E_a}, p_{I_c}, p_{I_a}, p_{C_c}, p_{C_a}, p_{R_c}, p_{R_a}$. Define the Hamiltonian

$$\begin{aligned}
\mathcal{H} = {} & I_c + I_a + \tfrac{w_1}{2}u_1^2 + \tfrac{w_2}{2}u_2^2 + \tfrac{w_3}{2}u_3^2\\
& + p_{S_c}\dot{S}_c + p_{S_a}\dot{S}_a + p_{V_c}\dot{V}_c + p_{V_a}\dot{V}_a + p_{E_c}\dot{E}_c + p_{E_a}\dot{E}_a\\
& + p_{I_c}\dot{I}_c + p_{I_a}\dot{I}_a + p_{C_c}\dot{C}_c + p_{C_a}\dot{C}_a + p_{R_c}\dot{R}_c + p_{R_a}\dot{R}_a,
\end{aligned}$$

where $\dot{X}$ are the right-hand sides of (37).

The adjoint system is given by

$$\dot{p}_X(t) = -\frac{\partial\mathcal{H}}{\partial X}, \qquad p_X(T) = 0,$$

for each state X. Below we display the adjoint equations (computed formally). For brevity we use the notation

$$\Phi(t) := \frac{I_c+\eta_c C_c+I_a+\eta_a C_a}{N}, \qquad \Psi(t) := \frac{I_a+\eta_v C_a}{N_a},$$

so that $\lambda_c = \beta_c\Phi,\ \lambda_a = \beta_a\Phi,\ \lambda_v = p_v\Psi$.

$$\dot{p}_{S_c} = -\Big[- p_{S_c}(\lambda_c + \theta_c + k_1u_1 + \rho + \mu) + p_{S_c}\Big(\frac{\partial \lambda_c}{\partial S_c}S_c\Big) + p_{V_c}(\theta_c + k_1u_1) + p_{E_c}\lambda_c\Big]$$

$$\dot{p}_{S_a} = -\Big[- p_{S_a}(\lambda_a + \theta_a + k_2u_2 + \mu) + p_{V_a}(\theta_a + k_2u_2) + p_{E_a}\lambda_a\Big]'_{S_a}$$

$$\dot{p}_{V_c} = -\Big[p_{S_c}\omega - p_{V_c}(\omega + \rho + \mu)\Big]$$

$$\dot{p}_{V_a} = -\Big[p_{S_a}\omega - p_{V_a}(\omega + \mu)\Big]$$

$$\dot{p}_{E_c} = -\Big[p_{E_c}(-(\sigma_c + \rho + \mu)) + p_{I_c}\sigma_c + p_{E_a}\rho + p_{E_c}\cdot\partial_{E_c}(\lambda_c S_c + \lambda_v(\phi + k_3u_3)\Lambda)\Big]$$

$$\dot{p}_{E_a} = -\Big[p_{E_a}(-(\sigma_a + \mu)) + p_{I_a}\sigma_a + p_{E_a}\cdot\partial_{E_a}(\lambda_a S_a)\Big]$$

$$\dot{p}_{I_c} = -\Big[1 + p_{I_c}(-(\gamma_c + \nu_c + \rho + \mu)) + p_{C_c}\nu_c + \sum_X p_X\partial_{I_c}\Big]$$

$$\dot{p}_{I_a} = -\Big[1 + p_{I_a}(-(\gamma_a + \nu_a + \mu)) + p_{C_a}\nu_a + p_{E_c}\cdot\partial_{I_a}(\lambda_v(\phi + k_3u_3)\Lambda) + \sum_X p_X\partial_{I_a}\Big]$$

$$\dot{p}_{C_c} = -\Big[p_{C_c}(-(\alpha_c + \rho + \mu + \delta_c)) + p_{R_c}\alpha_c + \sum_X p_X\partial_{C_c}\Big]$$

$$\dot{p}_{C_a} = -\Big[p_{C_a}(-(\alpha_a + \mu + \delta_a)) + p_{R_a}\alpha_a + p_{E_c}\cdot\partial_{C_a}(\lambda_v(\phi + k_3u_3)\Lambda) + \sum_X p_X\partial_{C_a}\Big]$$

$$\dot{p}_{R_c} = -\Big[- p_{R_c}(\rho + \mu) + p_{R_a}\rho\Big]$$

$$\dot{p}_{R_a} = -\Big[- p_{R_a}\mu\Big].$$

The terms "$\sum_X p_X\partial_{I_c}$" etc. above denote contributions from the dependence of $\lambda_c, \lambda_a, \lambda_v$ on I_c, I_a, C_c, C_a. Computing these explicitly yields (for instance)

$$\frac{\partial \lambda_c}{\partial I_c} = \beta_c\frac{N - (I_c + \eta_cC_c + I_a + \eta_aC_a)}{N^2}$$

and similarly for other partials; substitute into the adjoint ODEs for full explicit formulas.

5.2 Characterization of optimal controls

The optimal controls $u_i^*(t)$ minimise $\mathcal{H}$ a.e.; differentiating $\mathcal{H}$ with respect to each control and setting to zero gives the interior characterizations.

Control u_1. Only S_c and V_c depend linearly on u_1 through terms $(\theta_c + k_1u_1)S_c$ and $-(\theta_c + k_1u_1)S_c$. Thus

$$\frac{\partial \mathcal{H}}{\partial u_1} = w_1u_1 + k_1S_c\big(p_{V_c} - p_{S_c}\big).$$

Therefore the unconstrained minimiser is

$$u_1^\dagger(t) = -\frac{k_1S_c(t)\big(p_{V_c}(t) - p_{S_c}(t)\big)}{w_1},$$

and projecting to the admissible set $[0, 1]$ yields

$$u_1^*(t) = \min\Big\{1,\ \max\Big\{0,\ -\frac{k_1S_c(t)\big(p_{V_c}(t) - p_{S_c}(t)\big)}{w_1}\Big\}\Big\}. \tag{39}$$

Control u_2. Similarly,

$$\frac{\partial \mathcal{H}}{\partial u_2} = w_2 u_2 + k_2 S_a \big(p_{V_a} - p_{S_a}\big),$$

so

$$u_2^*(t) = \min\Big\{1,\ \max\Big\{0,\ -\frac{k_2 S_a(t)\big(p_{V_a}(t) - p_{S_a}(t)\big)}{w_2}\Big\}\Big\}. \tag{40}$$

Control u_3. The control u_3 appears in the newborn split and in the vertical infection term $\lambda_v(\phi + k_3 u_3)\Lambda$. Differentiation gives

$$\frac{\partial \mathcal{H}}{\partial u_3} = w_3 u_3 + k_3 \Lambda \big(p_{V_c} - p_{S_c}\big) + k_3 \Lambda\, p_{E_c}\, \lambda_v',$$

where $\lambda_v' = \partial_{(\phi + k_3 u_3)}\big(\lambda_v(\phi + k_3 u_3)\big) = p_v \frac{I_a + \eta_v C_a}{N_a} = p_v \Psi$. Neglecting the smaller second-order contribution from $\partial \lambda_v / \partial(\phi + k_3 u_3)$ (or including it explicitly if desired), a practical characterization is

$$\frac{\partial \mathcal{H}}{\partial u_3} \approx w_3 u_3 + k_3 \Lambda \big(p_{V_c} - p_{S_c}\big),$$

hence

$$u_3^*(t) = \min\Big\{1,\ \max\Big\{0,\ -\frac{k_3 \Lambda \big(p_{V_c}(t) - p_{S_c}(t)\big)}{w_3}\Big\}\Big\}, \tag{41}$$

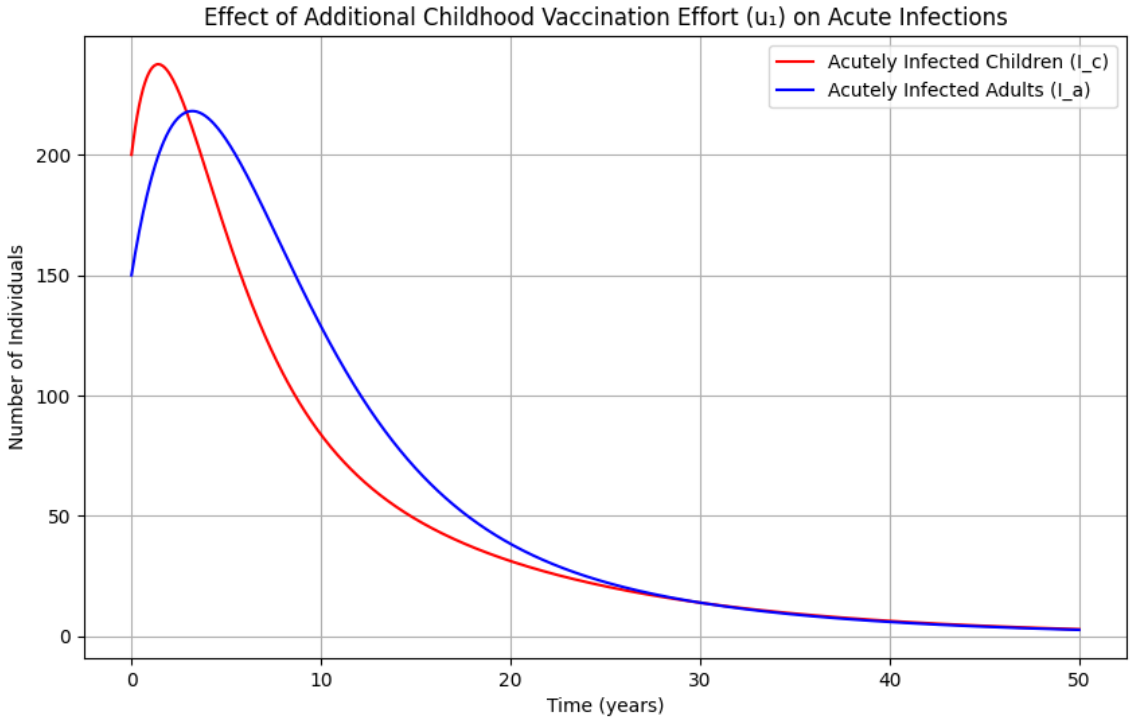

Figure 2: Effect of Additional Childhood Vaccination Effort (u_1) on Acute Infections

Figures 2 and 3 illustrate the impact of an increased effort in childhood vaccination (u_1) on acute infections and the control profile associated with this effort. The graphs depict the temporal dynamics of acute Hepatitis B infections among both children (I_c, red line) and adults (I_a, blue line) in the context of a time-varying childhood vaccination strategy. Both groups experience moderate and relatively stable levels of acute infections, indicative of the baseline endemic equilibrium of HBV in the absence of

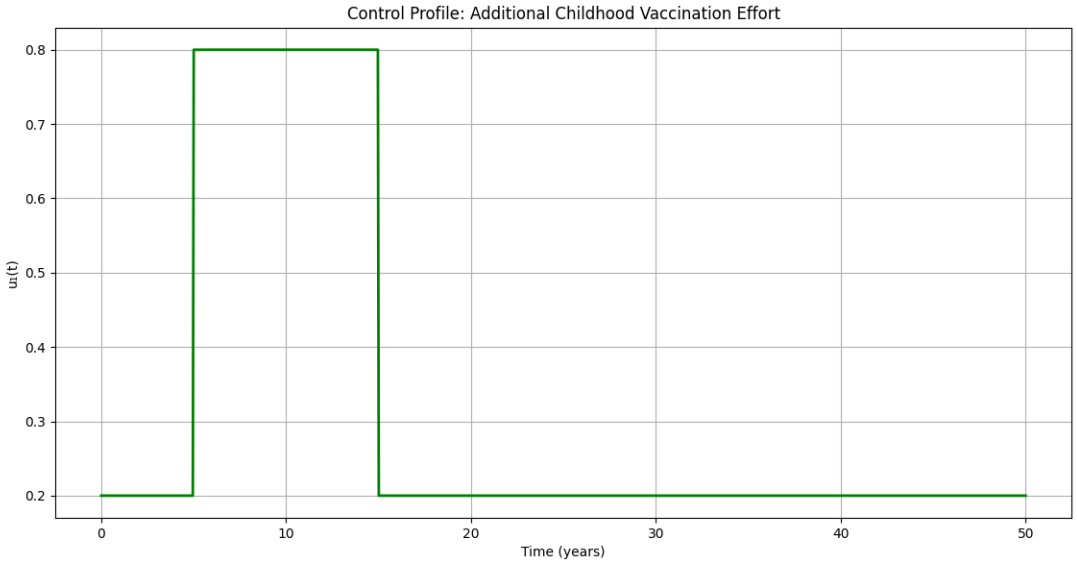

Figure 3: Control Profile of Additional Childhood Vaccination Effort

enhanced interventions. The higher initial value of I_c indicates ongoing transmission within the child population.

An immediate decline in childhood infections is observed when u_1 rises to 0.8 at year 5, resulting in a rapid and significant reduction in I_c. In contrast, I_a begins to decrease at a more gradual pace, reaching its lowest level around years 10 to 12. This suggests that the increased vaccination effort directly reduces the number of susceptible children, leading to an immediate decrease in new infections among this group. The decline in adult infections occurs via two mechanisms: the reduction of future infections as vaccinated children grow into adulthood, and the indirect effects of herd immunity, which limit transmission to adults. As u_1 falls back to 0.2 at year 15, I_c starts to rise sharply again.

The control profile graph outlines the public health strategy for intensifying childhood vaccination over time. A value of $u_1 = 0.2$ corresponds to routine vaccination efforts, which provide some degree of control but are not sufficient for a significant long-term reduction in disease burden. The square-wave pattern in the graph reflects a structured, time-limited public health campaign. The abrupt transitions indicate specific start and end dates for organized initiatives, rather than gradual changes. The return to baseline levels after year 15 suggests fluctuations related to funding cycles.

Ultimately, this indicates that childhood vaccination delivers immediate direct protection to children while providing delayed indirect protection to adults through decreased transmission and cohort effects. The rapid rebound in infections when control measures are relaxed emphasizes that managing infectious diseases requires ongoing efforts since temporary measures result in only short-term benefits. The differing response patterns observed between children and adults underscore the need for age-specific modeling in HBV, as transmission dynamics and the effects of interventions can vary among age groups. The successful reductions achieved during the intervention period demonstrate the potential effectiveness of intensified childhood vaccination efforts, indicating that scaling up routine programs could lead to significant public health improvements. Figure 4 illustrates a comparison of four trajectories over a 30-year period: (dashed red) Acute adult infections without control, (solid red) Acute adult infections with $u_2 = 1$ control, (dashed blue) Chronic adult infections without control, and (solid blue) Chronic adult infections with $u_2 = 1$ control. All four lines originate from initial conditions and display immediate divergence. The solid red line (I_a ctrl) shows a sharp decline due to direct protection for susceptible adults. The solid blue line (C_a ctrl) decreases more gradually, reflecting the development of chronic cases from existing acute infections. The dashed lines indicate ongoing natural transmission patterns. The controlled trajectories stabilize at lower levels, whereas

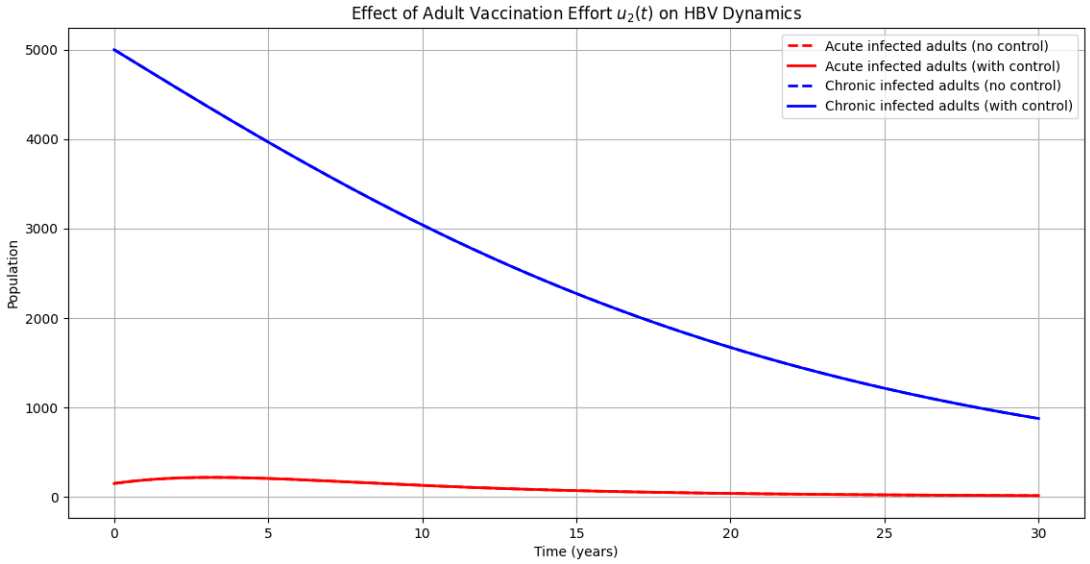

Figure 4: Effect of Adult Vaccination Effort $u_2(t)$ on HBV Dynamics

uncontrolled trajectories may reach an endemic equilibrium or experience gradual changes. Controlled trajectories achieve new stable equilibria significantly lower than the levels seen in uncontrolled scenarios. Despite the control measures, chronic infections (solid blue) persist due to slow clearance rates $(\alpha_a = 0.04year)$, continued progression from acute cases $(\nu_a = 0.05year)$, and aging of child chronic cases (ρC_c). The difference between the solid and dashed lines indicates immediate benefits for vaccinated individuals, herd effects that reduce community transmission, and the inability to eliminate the disease due to sustained child transmission and chronic reservoirs. Thus, the graph indicates that adult catch-up vaccination can significantly diminish the HBV burden.

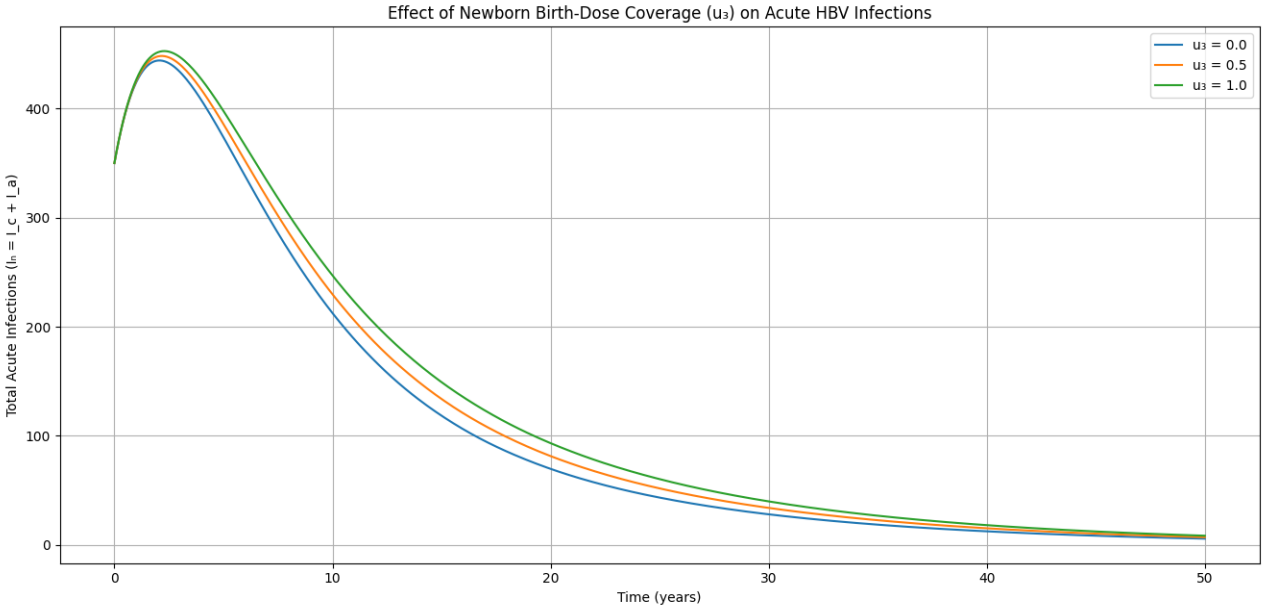

Figure 5: Effect of Newborn Birth-Dose Coverage (u_3) on Acute HBV Infections

Figure 5 depicts three infection trajectories over 50 years, each illustrating total acute infections (children + adults) under different levels of birth-dose coverage enhancement. All three lines begin

together but quickly diverge. An increase in u_3 immediately halts mother-to-child transmission. More vaccinated newborns lead to a reduction in future susceptible children. In contrast to interventions addressing existing infections, the birth-dose impacts the entry point of infections. The curves show a distinct separation, with $u_3 = 1.0$ displaying the steepest decline. Each trajectory stabilizes at a different level: $u_3 = 0.0$ indicates an endemic equilibrium sustained by ongoing transmission, $u_3 = 0.5$ reflects a significant reduction with persistent low-level transmission, and $u_3 = 1.0$ suggests near-elimination levels, potentially achieving disease control targets. Birth-dose vaccination is a genuine primary prevention method: it blocks infections at their origin rather than treating established disease, guards against the development of chronic carriers by providing protection prior to exposure, and represents the most efficient intervention per administered dose. This graph effectively illustrates that newborn birth-dose vaccination is the most essential intervention for HBV. The considerable separation between control levels clarifies why the WHO recommends achieving at least 90% HepB-BD coverage as crucial for elimination. Unlike interventions that target existing infections, u_3 prevents new infections at their source, offering sustainable protection that accumulates over generations. The biological analysis indicates that birth-dose coverage yields the highest return on investment and is fundamental to comprehensive HBV control strategies. The trajectory approaching near-elimination with $u_3 = 1.0$ emphasizes the critical need for universal birth-dose coverage, especially in high-endemic regions such as Nigeria.

6 Numerical analysis

The model simulation begins with an assumed total human population distributed between children and adults. At time $t = 0$, most individuals are susceptible, with small proportions vaccinated, exposed, infected, or recovered. These initial values are chosen to reflect typical epidemiological conditions for Hepatitis B in Nigeria, based on national demographic proportions and reported prevalence estimates.

Let the initial state variables be represented as:

$$(S_c(0), V_c(0), E_c(0), I_c(0), C_c(0), R_c(0), S_a(0), V_a(0), E_a(0), I_a(0), C_a(0), R_a(0))$$

$$\begin{aligned} S_c(0) &= 250{,}000, & V_c(0) &= 100{,}000, & E_c(0) &= 500, \\ I_c(0) &= 200, & C_c(0) &= 2{,}000, & R_c(0) &= 10{,}000, \\ S_a(0) &= 500{,}000, & V_a(0) &= 80{,}000, & E_a(0) &= 300, \\ I_a(0) &= 150, & C_a(0) &= 5{,}000, & R_a(0) &= 50{,}000. \end{aligned}$$

corresponding to the compartments of susceptible, vaccinated, exposed, acutely infected, chronically infected, and recovered individuals for children and adults respectively.

The specific numerical values used for simulation are based on the total population distribution and existing HBV data for Nigeria, ensuring biological realism and consistency with published studies.

Here is a table of parameter values and estimates informed by Nigerian HBV data and literature:

Table 3: Model parameters, descriptions, values, and sources for the age-structured Hepatitis B model in Nigeria.

Parameter	Description	Value	Citation
Λ	Recruitment (birth) rate	3.5×10^4 individuals/year	[1]
μ	Natural death rate	$1/65$ year^{-1}	[1]
ρ	Aging rate from children to adults	$1/15$ year^{-1}	Model assumption
β_c	Effective contact rate for children	3.0×10^{-4} year^{-1}	[18]
β_a	Effective contact rate for adults	2.8×10^{-4} year^{-1}	[19]
η_c	Relative infectiousness of chronic carriers (children)	0.8	[20]
η_a	Relative infectiousness of chronic carriers (adults)	0.9	[20]
ϕ	Hepatitis B birth dose coverage	0.70	[1]
θ_c	Routine vaccination rate for children	0.85 year^{-1}	[1]
θ_a	Catch-up vaccination rate for adults	0.25 year^{-1}	[18]
ω	Waning rate of vaccine-induced immunity	0.02 year^{-1}	[19]
σ_c	Progression rate from exposed to acute (children)	0.30 year^{-1}	[21]
σ_a	Progression rate from exposed to acute (adults)	0.25 year^{-1}	[21]
γ_c	Recovery rate from acute (children)	0.25 year^{-1}	[19]
γ_a	Recovery rate from acute (adults)	0.20 year^{-1}	[19]
ν_c	Progression to chronic (children)	0.10 year^{-1}	[22]
ν_a	Progression to chronic (adults)	0.05 year^{-1}	[22]
α_c	Recovery from chronic (children)	0.05 year^{-1}	[19]
α_a	Recovery from chronic (adults)	0.04 year^{-1}	[19]
δ_c	Disease-induced death (children)	0.01 year^{-1}	[19]
δ_a	Disease-induced death (adults)	0.015 year^{-1}	[19]
p_v	Vertical transmission probability	0.30	[20]
η_v	Relative risk of vertical transmission	0.80	[20]

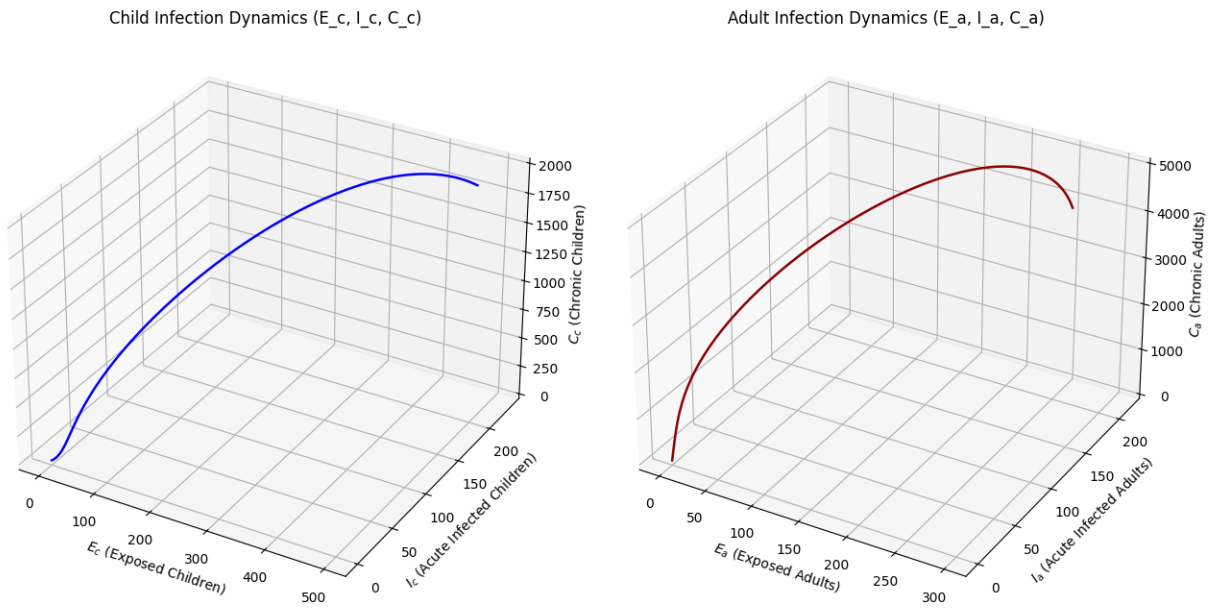

Figure 6: Child and Adult Infection Dynamics (E_a, I_a, C_a)

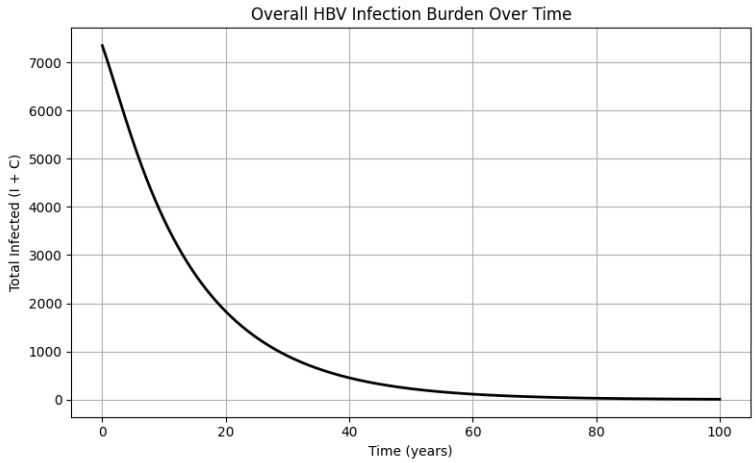

Figure 7: Overall HBV Infection Burden Over Time

Figure 6 illustrates the 3D trajectory of Hepatitis B infection progression through various stages within the child population over time. The three axes are defined as follows: X-axis (E_c) represents exposed children—those infected but not yet infectious (latent period); Y-axis (I_c) denotes acute infected children—those experiencing active, symptomatic infection; and Z-axis (C_c) reflects chronic carrier children—those who have developed a persistent infection. The trajectory likely begins with rapid movement as the initial exposed population $(E_c = 500)$ transitions to acute infection $(I_c = 200)$ and further develops into chronic carriers $(C_c = 2,000)$. This trajectory illustrates the natural history of HBV in children, demonstrating their movement from exposed to acute to chronic states. The relatively high $\nu_c(0.10year)$ indicates a substantial proportion of infected children progressing to chronic carriers. Additionally, children's chronic progression rates are typically higher than those of adults due to their immature immune systems. Over time, the trajectory stabilizes, suggesting that the system attains a steady state where new infections balance recoveries and aging out of the child compartment. The large C_c component signifies the significant burden of chronic HBV in children, who are at an increased risk of developing lifelong infections, cirrhosis, and liver cancer.

The second 3D graph in Figure 6 depicts HBV progression in the adult population, revealing no-

table differences compared to children: X-axis (E_a) identifies exposed adults, Y-axis (I_a) represents acute infected adults, and Z-axis (C_a) shows chronic carrier adults. The adult trajectory indicates more gradual transitions between states, a lower chronic carrier burden relative to acute infections, and the influence of aging inflows from child compartments. This suggests that adults contribute meaningfully to transmission due to longer infectious periods and higher contact rates in certain environments. Both trajectories represent a 100-year simulation that demonstrates how HBV achieves endemic equilibrium in a population under specified vaccination and transmission parameters. The spiral or curved characteristics of these trajectories illustrate the dynamic interactions between different infection states as the system progresses from initial conditions toward its long-term equilibrium state.

Figure 7 presents a 2D line plot depicting the total number of infected individuals $(I + C)$ across both children and adult populations over a century. The vertical axis indicates the combined burden of acute infections $(I_c + I_a)$—individuals with active, symptomatic Hepatitis B—and chronic carriers $(C_c + C_a)$—individuals with persistent, lifelong infections. This serves as an essential public health indicator, reflecting the total number of infectious individuals in the population at any given moment. The horizontal axis demonstrates the long-term dynamics of Hepatitis B over a hundred years and allows for the observation of how the infection burden evolves from initial conditions to equilibrium. This illustrates the effectiveness of HBV transmission through the population and indicates whether control measures are sufficient. Ultimately, this single graph offers a broad overview of the population-level impact of Hepatitis B and the efficacy of control strategies across generations.

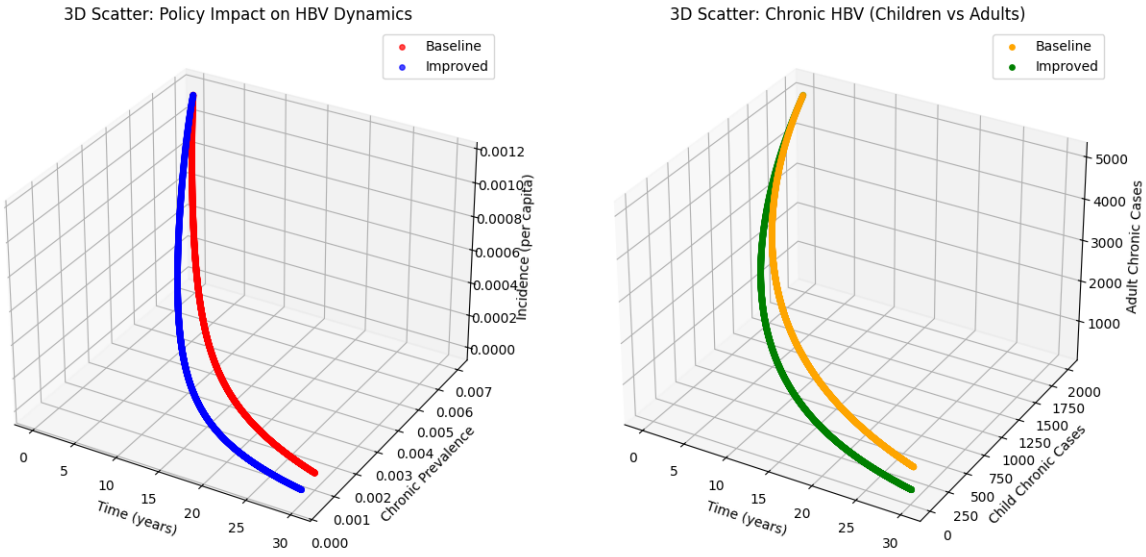

Figure 8: Policy Impact on HBV Dynamics and Chronic HBV (Children vs Adults)

Figure 8 presents two distinct 3D plots. The first 3D scatter graph illustrates the impact of policy on HBV dynamics. The X-axis represents time, indicating disease progression over a 30-year period. The Y-axis shows chronic prevalence, which refers to the proportion of the population with chronic HBV infection. The Z-axis reflects incidence, representing the rate of new infections in the population. The trajectory displays how chronic prevalence and incidence change together over time. The baseline, depicted in red, corresponds to current vaccination and treatment policies, while the improved scenario, shown in blue, illustrates the potential impact of the WHO 2030 targets with enhanced interventions. The ideal outcome would involve movement toward the origin, depicting both low prevalence and low incidence, with the improved scenario expected to demonstrate a faster decline toward lower values in both dimensions.

The second graph depicts chronic HBV cases among children and adults. The X-axis again represents a 30-year timeline, while the Y-axis displays the number of child chronic cases and the Z-axis reflects the number of adult chronic cases. This graph indicates the age distribution of the chronic HBV

burden over time. The baseline is represented in orange, reflecting the current distribution pattern, and the improved scenario is shown in green, indicating the distribution under enhanced interventions. There is a more rapid reduction in child cases due to improved birth dose and childhood vaccination, whereas the reduction in adult cases is slower because of the persistence of existing chronic infections. The trajectory should also move toward the origin, indicating fewer cases in both age groups. These graphs illustrate how coordinated vaccination strategies can effectively reduce both new infections (incidence) and long-term disease burden (chronic prevalence) across various age groups, contributing to HBV elimination goals. The 3D visualization effectively highlights the multifaceted nature of HBV control, where time, disease burden, and age distribution must all be considered when assessing the effectiveness of interventions.

7 Summary and Conclusion

7.1 Summary

This study developed an age-structured deterministic model to describe the transmission dynamics of Hepatitis B Virus (HBV) in Nigeria, incorporating both vertical (mother-to-child) and horizontal (person-to-person) transmission pathways. The model stratifies the population into children and adults, recognizing age-dependent differences in infection progression, immunity, and vaccine response. To ensure biological realism, the non-negativity of solutions and the existence of an invariant region were established, confirming that the system remains epidemiologically meaningful for all time.

The disease-free equilibrium (DFE) was derived and analyzed for stability using the Jacobian matrix, while the basic reproduction number (R_0) was computed via the next-generation matrix method. Analytical results revealed that when $R_0 < 1$, the DFE is both locally and globally asymptotically stable, verified using the Castillo–Chavez and Song approach. Conversely, when $R_0 > 1$, infection persists, and the endemic equilibrium was shown to be globally stable through the construction of an appropriate Lyapunov function, signifying the long-term persistence of HBV under endemic conditions.

An optimal control analysis was performed to evaluate the impact of three time-dependent interventions: childhood vaccination (u_1), adult catch-up vaccination (u_2), and birth-dose vaccination (u_3). The associated objective functional minimized infection prevalence and control costs. Numerical simulations provided insights into the temporal and structural dynamics of HBV transmission under different control scenarios.

Figures 2 and 3 demonstrated that intensifying childhood vaccination (u_1) significantly reduces acute infections among children, with a delayed but notable decline in adult infections due to indirect herd protection. However, the resurgence of infections following reduced control efforts highlights the necessity for sustained intervention programs. Figure 4 compared adult infection trajectories under varying control levels, revealing that adult catch-up vaccination (u_2) can markedly lower both acute and chronic infections, though complete eradication remains limited by slow clearance rates and persistent child-to-adult transmission.

Figure 5 examined the influence of birth-dose vaccination (u_3), demonstrating that higher coverage levels yield substantial declines in new infections, with $(u_3 = 1.0)$ approaching near-elimination conditions. This confirms the birth dose as the most effective strategy for interrupting vertical transmission and preventing chronic carrier formation. Figures 6 and 7 further visualized the infection trajectories within child and adult populations, showing the natural transition from exposure to chronic infection and the eventual stabilization at endemic equilibria. The simulations confirmed that children bear a disproportionate chronic burden due to immature immune responses, reinforcing the importance of early immunization.

Finally, Figure 8 illustrated policy-driven dynamics, showing that achieving the WHO 2030 HBV elimination targets would accelerate declines in both incidence and chronic prevalence. Improved vaccination strategies not only reduce new infections but also shift the chronic burden away from future generations.

In summary, the analysis and simulations demonstrate that comprehensive age-specific vaccination—particularly universal birth-dose and sustained childhood immunization—remains the most effective and cost-efficient strategy for HBV elimination in Nigeria. The model provides a robust analytical and computational framework to guide public health planning, ensuring long-term control and potential eradication of HBV across all age strata.

7.2 Conclusion

This research has developed and analyzed a deterministic model structured by age for the transmission dynamics of Hepatitis B Virus (HBV) in Nigeria, considering both vertical and horizontal transmission pathways. The theoretical foundation of the model was established through the derivation of an invariant region, confirmation of the non-negativity of solutions, and a comprehensive stability analysis. The calculation of the basic reproduction number R_0 provided an important epidemic threshold, with analytical results indicating that the Disease-Free Equilibrium (DFE) is locally and globally asymptotically stable when $R_0 < 1$, while the Endemic Equilibrium is globally stable when ($R_0 > 1$), highlighting the model's effectiveness in illustrating the persistent nature of HBV in endemic contexts.

The numerical simulations provided important public health insights, emphasizing the unique and combined functions of various vaccination strategies:

1. **Childhood Vaccination** (u_1)**:**The results indicate that increasing routine childhood vaccination offers immediate protection to children, as shown by the significant decrease in acute child infections (I_c). The more gradual reduction in adult infections (I_a) highlights the strong, delayed cohort effect and herd immunity resulting from this initiative. Nevertheless, the rapid increase in infections following the end of a vaccination campaign clearly demonstrates that controlling HBV is not a short-term task; it necessitates ongoing, high-coverage vaccination programs to sustain long-term advantages.

2. **Adult Catch-up Vaccination** (u_2)**:** The implementation of adult vaccination results in a rapid decrease in acute infections among adults, providing direct protection to a significant group of transmitters. In contrast, its effect on the chronic adult carrier population (C_a) is more gradual, limited by the slow natural clearance rate and the continued progression of existing acute infections. This intervention notably decreases the overall disease burden, but it is not sufficient for complete elimination, as it does not tackle the reservoir of infection present in children and chronic carriers.

3. **Birth-Dose Vaccination** (u_3)**:** The analysis highlights birth-dose vaccination as the most effective single intervention for achieving HBV elimination. By preventing vertical transmission at its source, (u_3) serves as a primary prevention tool. The trajectory under complete birth-dose coverage $(u_3 = 1.0)$ approaches near-elimination levels, significantly changing the long-term course of the disease by stopping the formation of new chronic carriers from birth. This finding strongly supports the World Health Organization's focus on attaining high HepB-BD coverage as a fundamental aspect of HBV control.

The 3D and long-term trajectory plots clarify the complex natural history of HBV, illustrating the high rate of progression from acute to chronic states in children and the significant burden of chronic carriers. The century-long simulation of total infected individuals offers a realistic perspective on the disease's endemic persistence, while also indicating that coordinated interventions could significantly reduce this equilibrium.

This study indicates that a comprehensive, age-targeted strategy is necessary for addressing Hepatitis B in Nigeria. While catch-up vaccination for adults can lead to immediate decreases in transmission, vaccination in childhood provides important direct and herd protection. However, the universal and timely administration of the birth-dose vaccine appears to be the most effective and sustainable approach to disrupt the cycle of transmission and work towards the elimination of HBV as a public health

concern. The model functions as a useful resource for policymakers to simulate and optimize the allocation of limited resources for the greatest long-term benefit.

Acknowledgment

The authors, Frankline C. Eze and Martins U. Uwaezuoke, express their gratitude to the Department of Mathematics, Imo State University, Owerri for its support and guidance during this research. The feedback and insights from colleagues and reviewers improved the analytical rigor and clarity of this work.

The authors acknowledge the contributions of the mathematical epidemiology community, whose previous studies informed the formulation and analysis of key model components, such as the invariant region, non-negativity of solutions, disease-free equilibrium, and the computation of the basic reproduction number using the next-generation matrix method. They appreciate the theoretical frameworks used in the local stability analysis via the Jacobian method, the global stability of the disease-free equilibrium through the Castillo–Chavez and Song approach, and the global stability of the endemic equilibrium with the Lyapunov function technique.

The authors also recognize the significance of the World Health Organization (WHO) 2030 HBV elimination targets, which provided important context for understanding the model's optimal control results and policy implications.

References

[1] World Health Organization (2024). Hepatitis B. Retrieved April 9, 2024, from https://www.who.int/news-room/fact-sheets/detail/hepatitis-b

[2] Musa, B.M., Bussell, S., Borodo, M. M., Samaila, A. A., and Femi, O. L. (2015). Prevalence of hepatitis B virus infection in Nigeria, 2000–2013: A systematic review and meta-analysis. Nigerian Journal of Clinical Practice, 18(2), 163–172. https://doi.org/10.4103/1119-3077.151035

[3] Ezeanya, C.C., Okafor, I.M., and Udigwe, G.O. (2023). Sero-prevalence of hepatitis B surface antigen among pregnant women in a tertiary hospital in South-East Nigeria. Nigerian Journal of Medicine, 32(1), 45–50.

[4] Ott, J.J., Stevens, G.A., Groeger, J., and Wiersma, S.T. (2012). Global epidemiology of hepatitis B virus infection: New estimates of age-specific HBsAg seroprevalence and endemicity. Vaccine, 30(12), 2212–2219. https://doi.org/10.1016/j.vaccine.2011.12.116

[5] Ekpini, E., and Onyemelukwe, G.C. (2006). Hepatitis B virus infection in Nigeria: A review. Nigerian Medical Journal, 47(4), 9–14.

[6] Centers for Disease Control and Prevention (CDC). (2023). Hepatitis B Questions and Answers for Health Professionals. Retrieved October 31, 2023, from https://www.cdc.gov/hepatitis/hbv/hbvfaq.htm

[7] World Health Organization (2017). WHO Hepatitis B Fact Sheet. https://www.who.int/news-room/fact-sheets/detail/hepatitis-b

[8] National Primary Health Care Development Agency (NPHCDA). (2019). National Routine Immunization Strategic Plan 2019–2023. Government of Nigeria.

[9] World Health Organization (WHO)(2024). Immunization Data. Retrieved April 9, 2024, from https://www.who.int/teams/immunization-vaccines-and-biologicals/immunization-analysis-and-insights/global-monitoring/immunization-coverage

[10] Adekoya, B. J., Akinroye, K. K., Osibogun, A., and Odukoya, O. O. (2021). Barriers to the uptake of hepatitis B birth dose vaccine in Nigeria: A systematic review. Nigerian Journal of Clinical Practice, 24(8), 1121–1130. https://doi.org/10.4103/njcp.njcp_563_20

[11] Schweitzer, A., Horn, J., Mikolajczyk, R.T., Krause, G., and Ott, J.J. (2015). Estimations of worldwide prevalence of chronic hepatitis B virus infection: A systematic review of data published between 1965 and 2013. The Lancet, 386(10003), 1546–1555. https://doi.org/10.1016/S0140-6736(15)61412-X

[12] Okonkwo, U.C., Ojo, O.S., and Ndububa, D.A. (2022). Epidemiology of hepatocellular carcinoma in Nigeria: A review. Nigerian Journal of Gastroenterology and Hepatology, 14(1), 1–8.

[13] Pan, C.Q., and Duan, Z. (2022). Prophylaxis of hepatitis B virus recurrence after liver transplantation: A review. Hepatology International, 16(1), 23–39. https://doi.org/10.1007/s12072-021-10275-7

[14] World Health Organization (WHO). (2020). Prevention of Mother-to-Child Transmission of Hepatitis B Virus: Guidelines on Antiviral Prophylaxis in Pregnancy. https://www.who.int/publications/i/item/978-92-4-000270-8

[15] Ajayi, I.O., and Adewole, I.F. (2019). Hepatitis B virus infection among apparently healthy adults in Nigeria: A systematic review and meta-analysis. International Journal of Infectious Diseases, 83, 93–101. https://doi.org/10.1016/j.ijid.2019.04.011

[16] Van den Driessche, P., and Watmough, J. (2002). Reproduction numbers and sub-threshold endemic equilibria for compartmental models of disease transmission. Mathematical Biosciences, 180(1–2), 29–48.

[17] Castillo-Chavez, C., and Song, B. (2004). Dynamical models of tuberculosis and their applications. Mathematical Biosciences and Engineering, 1(2), 361–404.

[18] Akabuike, O.M., Aworh, M.K., Uzoebo, N.L., Erwat, J., Agukwe, O., Ngong, K., and Dangana, A. (2024). Evaluating hepatitis B screening, prevalence, vaccination coverage, and linkage to care in Abuja, Nigeria: Insights from a cross-sectional study. BMC Public Health, 24, 3475. https://doi.org/10.1186/s12889-024-17703-3

[19] Olakunde, B.O., Adeyinka, D.A., Olakunde, O.A., Eneh, S.C., and Ogundipe, T. (2025). Epidemiology of hepatitis B virus infection in Nigeria: A narrative review of prevalence, transmission, genotypes, coinfections, and mortality. Journal of Tropical Medicine, Article ID 4939367. https://doi.org/10.1155/2025/4939367

[20] Ndububa, D., Kuti, O., Awowole, I., Adekanle, O., Ijarotimi, O., Makinde, O., Anyabolu, C., and Ijadunola, M. (2022). Prospective cohort study of prevention of mother-to-child transmission of hepatitis B infection and 9 months follow-up of hepatitis B-exposed infants in Nigeria. BMJ Open, 12, e063482. https://doi.org/10.1136/bmjopen-2022-063482

[21] Onwuakor, C.E., Eze, V.C., Nwankwo, I.U., and Iwu, J.O. (2014). Sero-prevalence of hepatitis B surface antigen (HBsAg) amongst pregnant women attending antenatal clinic at the Federal Medical Centre Umuahia, Abia State, Nigeria. American Journal of Public Health Research, 2(6), 255–259. https://doi.org/10.12691/ajphr-2-6-7

[22] Uwandu, M.O., Okwuraiwe, A.P., and Ige, F.A. (2023). A four-year trend of acute hepatitis B virus infection at a tertiary health facility in Lagos, Nigeria. European Journal of Medical and Health Sciences, 5(1), 11–15. https://doi.org/10.24018/ejmed.2023.5.1.1945

[23] Anderson, R.M., and May, R.M. (1991). Infectious Diseases of Humans: Dynamics and Control. Oxford University Press, Oxford, UK.

[24] Edmunds, W.J., Medley, G.F., Nokes, D.J., Hall, A.J., and Whittle, H.C. (1993). The influence of age on the development of the hepatitis B carrier state. Proceedings of the Royal Society of London. Series B: Biological Sciences, 253(1337), 197–201. https://doi.org/10.1098/rspb.1993.0102

[25] Goyal, A., and Murray, J.M. (2022). The impact of vaccination and antiviral therapy on hepatitis B and hepatitis D epidemiology. PLOS ONE, 17(1), e0262577. https://doi.org/10.1371/journal.pone.0262577

[26] McDonald, S.A., van Leth, F., and de Wit, G.A. (2020). Mathematical modelling of viral hepatitis in Africa: A systematic review. Journal of Viral Hepatitis, 27(7), 644–653. https://doi.org/10.1111/jvh.13276

[27] Williams, J.R., Nokes, D.J., Medley, G.F., and Anderson, R.M. (1996). The transmission dynamics of hepatitis B in the UK: A mathematical model for evaluating costs and effectiveness of immunization programmes. Epidemiology & Infection, 116(1), 71–89. https://doi.org/10.1017/S0950268800058955